Carbon nanostructures

Wei-Li Lee, IoP, Academia Sinica

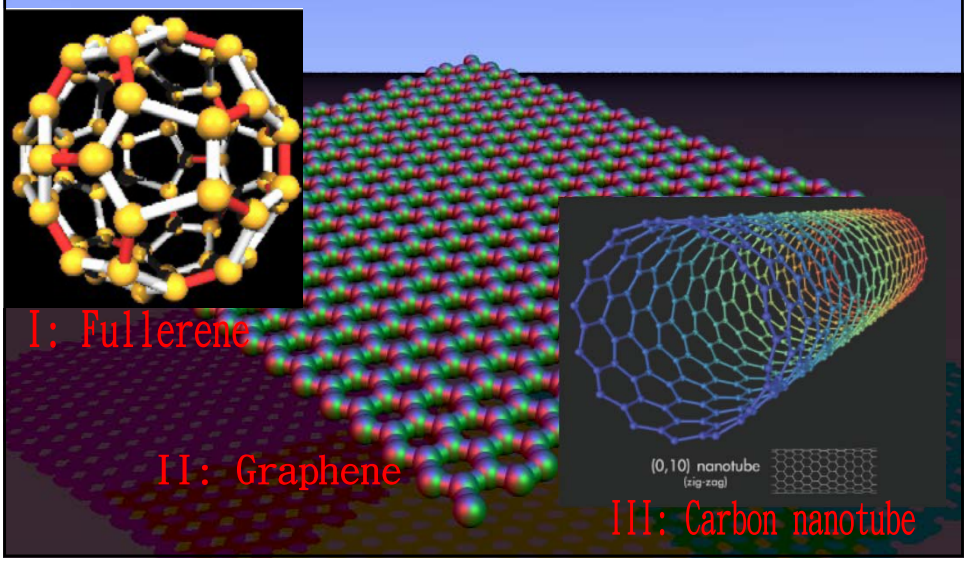

Welcome to Carbon World !!

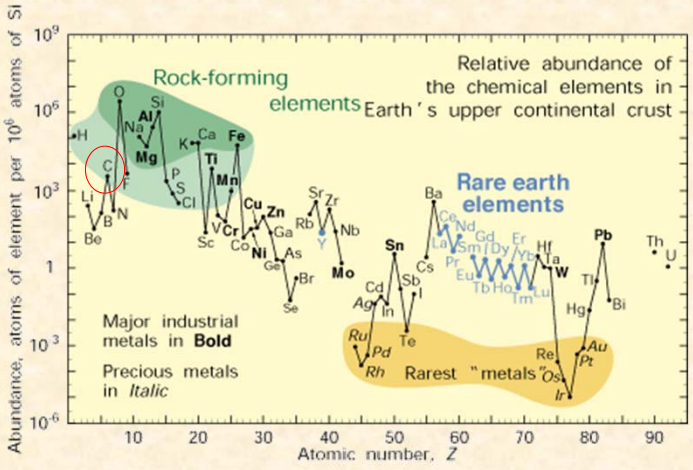

Wilkenson Microwave Anisotropy Probe

WMAP image of CMB (3 Kelvin)

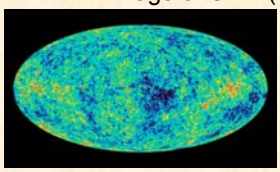

Angular spectrum

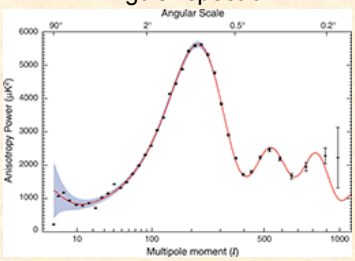

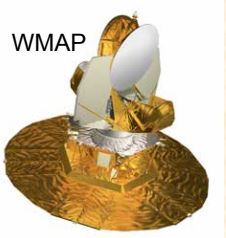

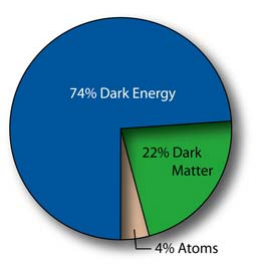

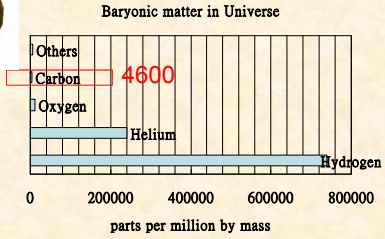

The Nobel Prize in Physics 1978

"for their discovery of cosmic microwave background radiation"

Discovery of Cosmic Background

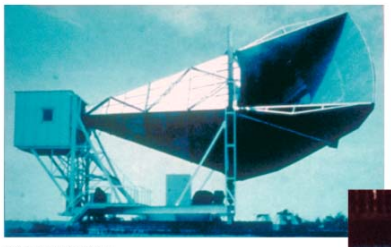

Microwave Receiver

Robert Wilson

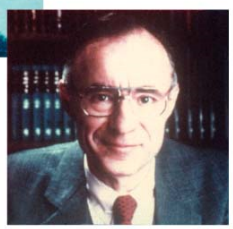

Arno Penzias

MAP990045

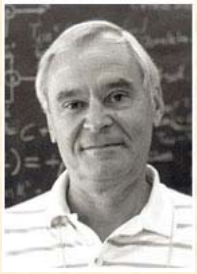

Dave Wilkinson

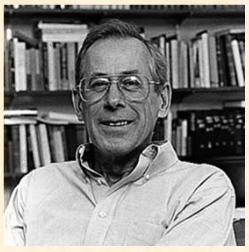

James Peebles

Carbon Bond : hybridized orbitals

• Carbon : atomic number 6, $1s^2$ [$2s^2$ $2px^1 2py^1$]

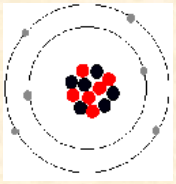

Molecular orbital :

$$\psi_j = \sum_i C_{ij} X_i$$

X_i : atomic orbitals

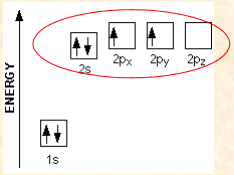

	Orbitals used for bond	Shape & bond angle	Examples:	
Sp	s, px	Digonal 180°	C_2H_2 Acetylene	H—C≡C—H
Sp^2	s, px, py	Trigonal 120°	Graphite, C_2H_4 Ethylene	
sp^3	s, px, py, pz	Tetrahedra 109°28'	Diamond, CH_4 Methane	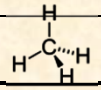

Allotropic forms in solid carbon

• **Many stable and known forms at R.T.**
Examples: diamond, graphite, amorphous carbon, fullerene, carbon nanotube and nanobud…etc

• **Two main structures :** one with sp^3 hybrid bonds (diamond) and the other with sp^2 hybrid bonds (graphite, fullerene, nanotube and nanobud)

• Dramatic different properties between diamond and graphite

	Diamond	**Graphite**
Electric	Insulator	Conductive
Hardness	10 (Mohs scale)	1-2
Appearance	Transparent	Opaque (black)
Value	Expensive	cheap

Structure of C_{60}

- European Football like molecule containing 60 carbons
  - 12 pentagonal and 20 hexagonal faces
  - Double bond length 1.4 Å and single bond 1.46 Å
- Named after architect R. Buckminster Fuller (1895-1983)

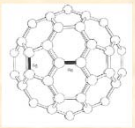

7.1 Å

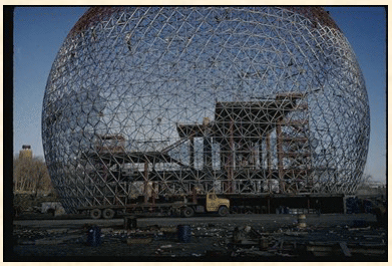

Geodesic dome

- Geometrically-allowed fullerene C_{20+h*2}

12 pentagonal faces + arbitrary number of hexagonal faces (h)

- Smallest Fullerene C_{20}
- Smallest isolated (stable) Fullerene C_{60}

Euler's theorem for polyhedral:

$f + v = e + 2, \quad f$: # of faces, v: # of vertices, e: # of edges

Discovery of Fullerene C_{60}

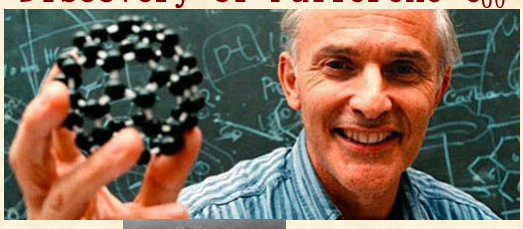

"An idea from outer space"
5.6 eV optical extinction

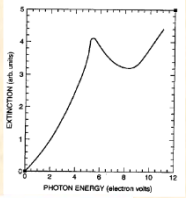

Harold Kroto
Univ. of Sussex
at Brighton UK

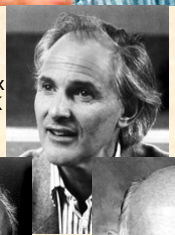

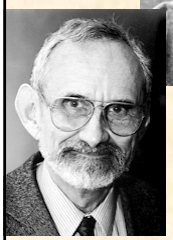

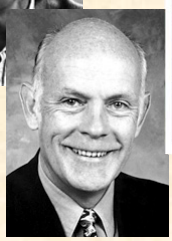

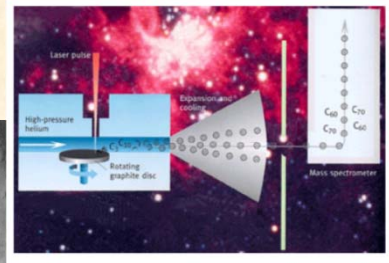

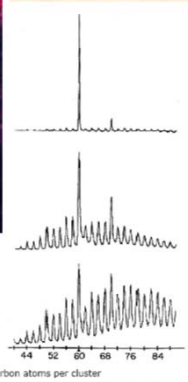

C60 and C70 clusters:
- Highly stable
- react weakly with gases

A molecule with great symmetry as a sphere

Robert Kurl, and Richard Smalley, Rice Univ. at Houston

Nobel Prize laureates in Chemistry 1996

Development of Fullerene

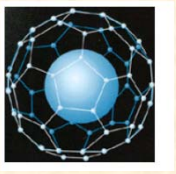

- Carbon ball with a metal core
- Mass production of Fullerene by astrophysicists D. R. Huffmann and W. Krätschmer
- Carbon nanotube – special electric and mechanical properties
- New superconducting crystals M_3C_{60}

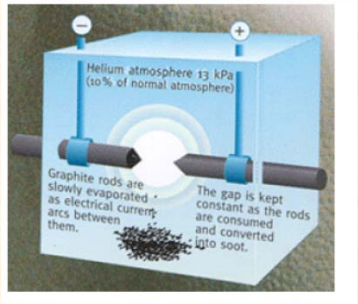

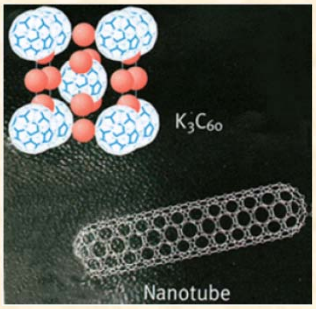

Adsorption of free-radicals(自由基) using Water-Soluble Fullerene C_{60}

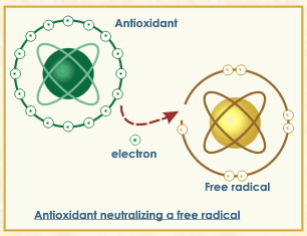

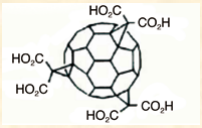

Water-soluble C_{60}

Free-radicals refer to atoms or molecules containing unpaired electrons at the surface. They are highly reactive and can cause damage to the cell or tissue by removing their electrons.

C_{60} can effectively bond to the free-radicals and has been used as an ingredient in anti-oxidant medicine.

Effect of size and dimensionality on electronic property

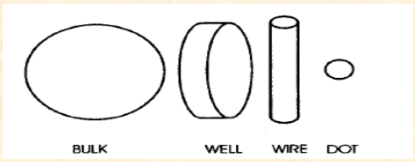

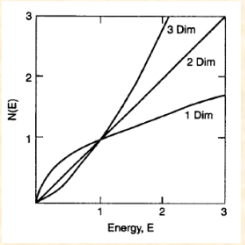

Table 9.4. Number of electrons *N* and density of states $D(E) = dN(E)/dE$ as a function of the energy *E* for conduction electrons delocalized in one, two, and three spatial dimensions[a]

Number of Electrons N	Density of States $D(E)$	Delocalization Dimensions
$N = K_1 E^{1/2}$	$D(E) = \frac{1}{2} K_1 E^{-1/2}$	1
$N = K_2 E$	$D(E) = K_2$	2
$N = K_3 E^{3/2}$	$D(E) = \frac{3}{2} K_3 E^{1/2}$	3

[a]The values of the constants K_1, K_2, and K_3 are given in Table A.2 (of Appendix A).

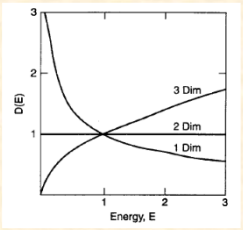

0-D quantum dot : an artificial atom

- quasi-0D system : d < ℓ_{mfp}

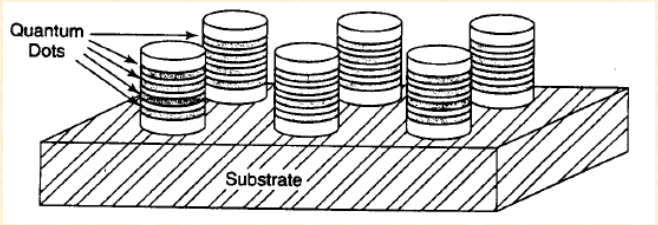

- Discrete energy level resembles the atomic level of a free atom
  - ex : 3-D infinite rectangular square well

$$E_n = \left(\frac{\pi^2\hbar^2}{2ma}\right)\left(n_x^2 + n_y^2 + n_z^2\right) = E_0 n^2$$

Quantum number = 0,1,2…

6 degeneracy (including spin) at ground state level E_o

Drude model (3-D):

$$\ell_{mfp}(\rho, n) = \frac{(3\pi^2)^{1/3}\hbar}{e^2\rho \cdot n^{2/3}}$$

- For a metal: n ~ 10^{23} cm^{-3} and ρ = 10^{-8} Ohm-m ℓ_{mfp}~ 59 nm
- For a semiconductor with n ~ 10^{16} cm^{-3} and ρ = 10^{-5} Ohm-m, ℓ_{mfp}~ 2,700 nm

Molecular orbital levels of a "free" C_{60}

- Shell model in a free fullerene : symmetry-based model
- 60 π-electrons filling the molecular level

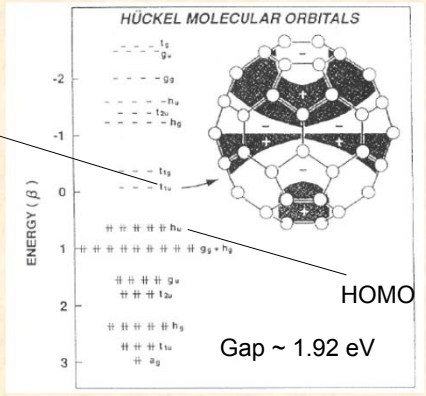

π energy states (in eV) of the C_{60} phenomenological Hamiltonian model.

ℓ	Symmetry	Model[a]	*Ab initio*[b]
0	a_g	−7.41	−7.41
1	f_{1u}	−6.87	−6.87
2	h_g	−5.87	−5.82
3	f_{2u}	−4.40	−4.52
	g_u	−4.13	−3.99
4	h_g	−2.21	−2.44
	g_g	−2.12	−2.37
5	h_u	−0.20	−1.27
	f_{1u}	0.88	0.62
	f_{2u}	1.82	2.71
6	f_{1g}	3.38	1.59
	h_g	3.43	2.78
	g_g	4.92	4.60

- Free C60 molecule should be a good insulator

Band structure of solid C_{60}

- Molecular crystal : BCC stacking structure
- Grown by slow evaporation from benzene solution filled with C60 molecules
- Band calculation :
  LDA + Gaussian orbital basis set
- Useful information :
  - Insulator with direct band gap ~ 1.5 eV band width ~ 0.4 eV
  - charge density map suggest weak coupling b/w fullerene molecule

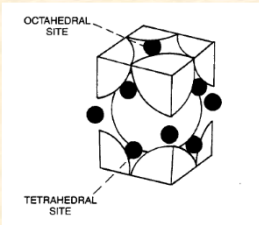

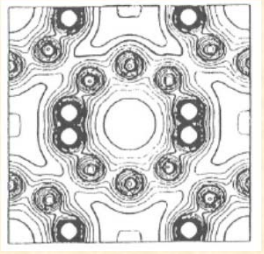

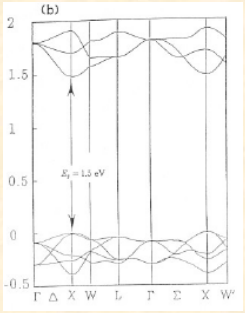

Symmetry consideration and Merohedral disorder in C_{60}

• Two standard orientations of fullerene molecule

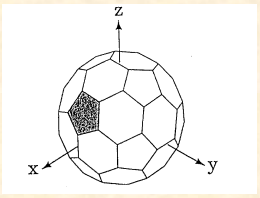

Two fold sym. axis

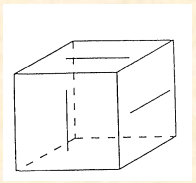

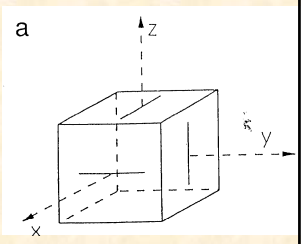

Two standard orientations

• Merohedral disorder : random choice b/w one of the two possible standard orientations (lack of four fold symmetry point)

➢ relative orientation b/w adjacent C_{60} can affect its physical properties.

Doping Buckyball solid : M_xC_{60}

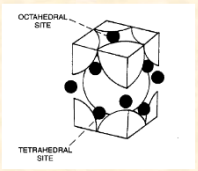

• Electrons transfer from alkali metal element M

• Two competing process due to doping effect:
- decrease of C_{60} wave func. overlap
- increase of the D.O.S

• Best conductivity occurs at x ~ 3 (half filled band)
-available sites (octahedral and tetrahedral) all filled

• undoped fullerene ρ_{300K}~ 10^8 Ωcm

• Single crystal K_3C_{60} ρ_{300K} ~ 5 mΩcm

• Strongly correlated electronics system
- $k_F\ell$ <1 , one electron model may fail
- from photo emission, large Hubbard U (1-2 eV)

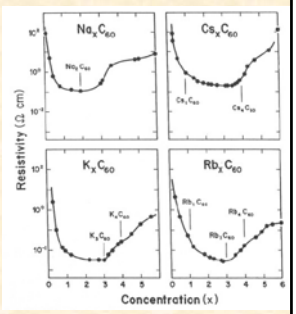

Drude model (3-D): $k_F\ell_{mfp}(\rho,n) = \frac{(3\pi^2)^{2/3}\hbar}{e^2\rho\cdot n^{1/3}}$ ~ 0.5 <1 for K_3C_{60}

Table 14.1

Physical constants for M_3C_{60} (M = K, Rb).

Quantity	K_3C_{60}	Rb_3C_{60}	Reference
Space group	$Fm\bar{3}$	$Fm\bar{3}$	[14.10]
C_{60}—C_{60} distance (Å)	10.06	10.20	[14.10]
M-C_{60} closest distance (Å)	3.27	3.33	[14.10]
Volume per C_{60} (cm^3)	7.22×10^{-22}	7.50×10^{-22}	[14.10]
fcc lattice constant a (Å)	14.253	14.436	[14.11]
$(-d \ln a/dP)$ (GPa^{-1})	1.20×10^{-2}	1.52×10^{-2}	[14.12]
Bulk modulus (GPa)	28	22	[14.13]
Thermal expansion coefficient (Å/K)	2×10^{-5}	—	[14.10]
Cohesive energy (eV)	24.2	—	[14.13]
Heat of formation (eV)	4.9	—	[14.13]
Density of states[a] [states/(eV/C_{60})]	25	35	[14.14]
Carrier density[a] ($10^{21}/cm^3$)	4.155	4.200	[14.10]
Electron effective mass (m_e)	1.3	—	[14.13]
Hole effective mass (m_e)	1.5, 3.4	—	[14.13]

[a] Assumes 3 electrons per C_{60}.

Calculated n = 2.07 x 10^{21} cm^{-3} for K_3C_{60}

Superconductivity in M_3C_{60}

- Discovered in K_3C_{60} by Hebard (Bell lab, 1991) T_c ~ 19.8 K
- Highest Tc ~ 33K in Cs_2RbC_{60}
- The larger the radius of the dopant alkali atom the higher the T_c

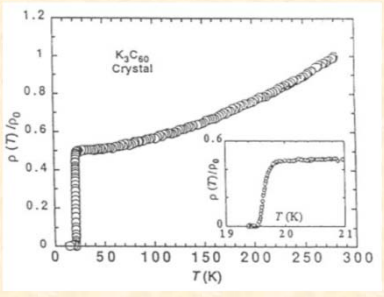

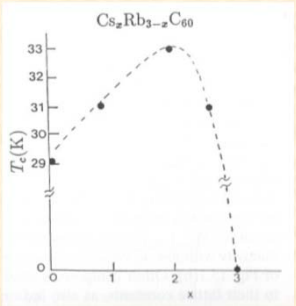

K_xC_{60}

X=0 (insulator) — 3 (superconductor) — 6 (insulator)

Strongly correlated electronic nature

Bardeen-Cooper-Schrieffer Theory

• In weak-coupling limit (λ <<1)

$$k_B T_c = 1.13\hbar\omega_D \exp[-1/\lambda],\ \lambda \equiv N(E_F)V$$

λ : dimentionless e - phonon coupling parameter

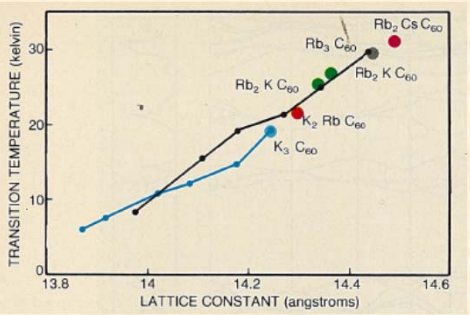

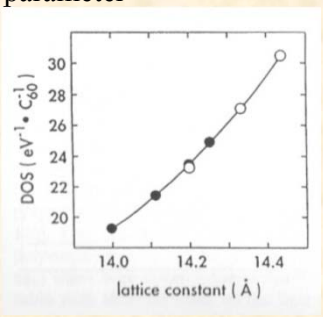

• Increase in lattice spacing reduced overlap of molecular orbital
⇨ reduced band width and increased D.O.S. $N(E_F)$

$$N(E_F) = \frac{3}{2}\frac{n}{E_F}$$

n fixed , lattice spacing ↑ k_F ↓ and $N(E_F)$ ↑

Pressure dependence of Tc

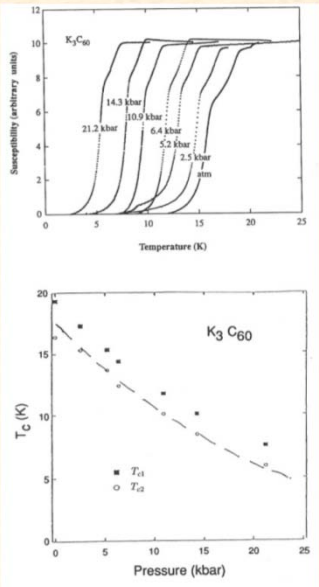

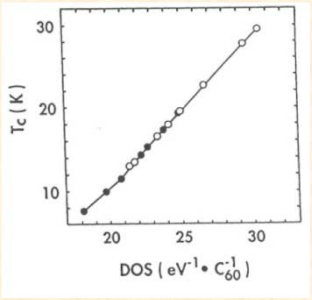

Fig. 15.3. Dependence of T_c on the density of states at the Fermi level for K_3C_{60} (closed circles) and Rb_3C_{60} (open circles) [15.22] using pressure-dependent measurements of T_c on these compounds [15.17, 23].

Other properties in K_3C_{60}

- Hall coefficient : $R_H = 1/ne$
  - ✓Sign change at 200K
  - ✓Both electron and hole like pockets

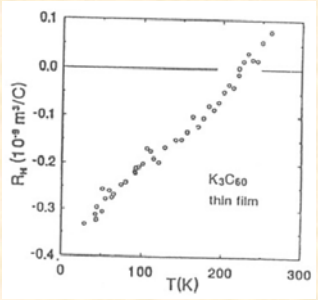

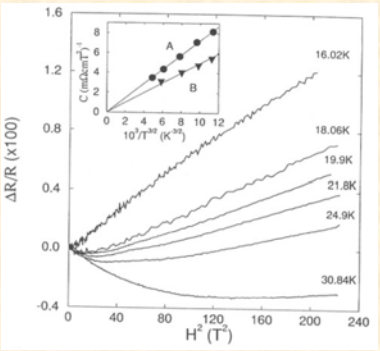

- Transverse magnetoresistance :

$$\frac{\Delta\rho}{\rho_0} = \frac{\Delta\rho_C}{\rho_0} + \frac{\Delta\rho_{L,I}}{\rho_0}$$

Classical orbital contribution : positive and quadratic in H

Weak localization and e-e interaction:

Negative, H^2 at low H and $H^{1/2}$ in high H

Weak localization in disordered system

- Appeared In disordered + time reversal symmetric system
- Negative MR : Strongly suppressed by applying magnetic field
- Merohedral disorder and also missing alkali ion at the tetrahedral and octahedral sites

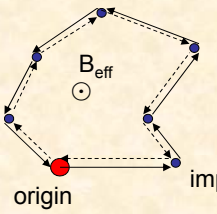

Constructive $|2A|^2$ ⇨ localization

$$\int B \cdot dA = \oint A \cdot d\ell : \text{additional phase change}$$

PartI: Concluding Remarks

- Fullerene structure : C_{20+h*2}
- An example of strongly correlated electronic system
  - Insulator – undoped C_{60}
  - Metallic – Alkali-doped C_{60}
  - Superconductivity – A_3C_{60} (A=K, Rb,CsK,RbCs)
- T_c increase linearly with lattice constant : BCS theory prediction
- Reduced Hall coefficient and sign change at 200K : both electron and hole pocket
- Weak localization effect associated with Merohedral disorder and missing alkali ions.
- D.O.S. at Fermi Level in K_3C_{60}:
  - Pauli susceptibility : 28 states/eV-C60(spin fluctuation enhancement
  - Thermopower S : 11 states/eV-C60
  - Specific heat : 12 states/eV-C60

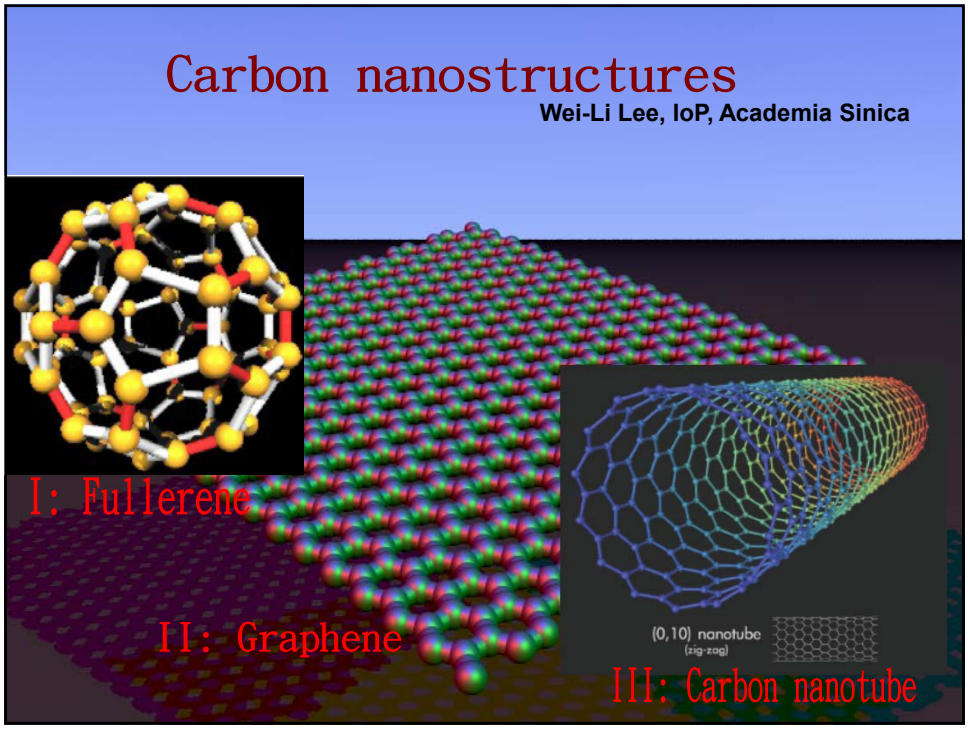

Part - 1

Basics of graphene

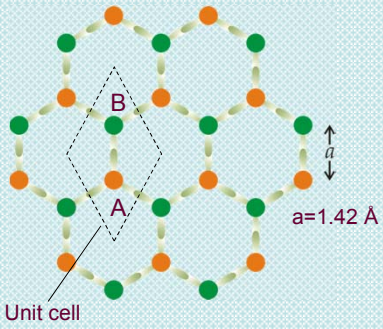

Honeycomb structure

- **Condensed-matter systems usually described accurately by the Schrödinger equation.**

$$i\hbar\frac{\partial}{\partial t}\psi(\vec{r},t)=\left(\frac{\vec{P}^2}{2m}+\vec{V}(\vec{r})\right)\psi(\vec{r},t)=E\psi(\vec{r},t)$$

- **Electron transport in graphene is governed by Dirac's (relativistic) equation.**

$$i\hbar\frac{\partial}{\partial t}\psi(\vec{r},t)=\left(\alpha_k p_k c+\beta mc^2\right)\psi(\vec{r},t)=\pm E\psi(\vec{r},t)$$

- **Charge carriers in graphene mimic relativistic particles with zero rest mass and effective speed of light $v_F \approx 10^6$m/s.**

- **Variety of unusual phenomena associated with massless Dirac fermions.**

Lattice structure

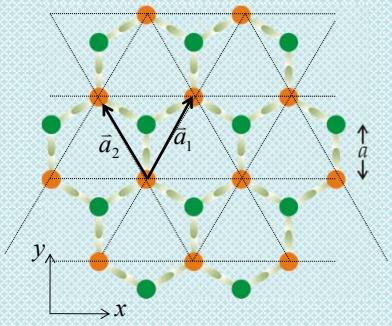

Triangular Bravais Lattice with basis of 2 carbon atoms

$$\vec{a}_i\cdot\vec{b}_j=2\pi\delta_{ij}$$

- **Triangular Bravais lattice :**

$$\vec{a}_1=a\sqrt{3}\left(\frac{1}{2},\frac{\sqrt{3}}{2}\right),\quad \vec{a}_2=a\sqrt{3}\left(-\frac{1}{2},\frac{\sqrt{3}}{2}\right)$$

- **Reciprocal Lattice :**

$$\vec{b}_1=\frac{2\pi}{3a}(\sqrt{3},1),\quad \vec{b}_2=\frac{2\pi}{3a}(-\sqrt{3},1)$$

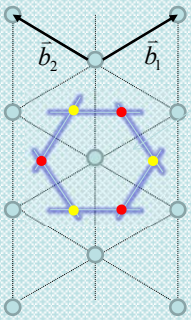

First Brillouin Zone with 6 vertices (Dirac points)

Electronic Structure : Tight Binding Model

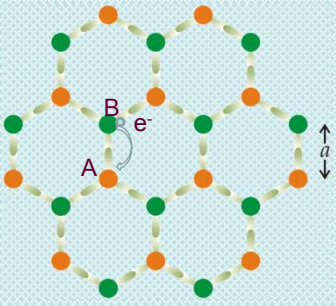

t : nearest neighbour hopping amplitude

- **Hamiltonian :**

$$H_{\text{int}} = -t \sum_{<i,j>,\sigma} \left[a^{+}_{i\sigma} b_{j\sigma} + H.C. \right]$$

$$-t' \sum_{<<i,j>>,\sigma} \left[(a^{+}_{i\sigma} a_{j\sigma} + b^{+}_{i\sigma} b_{j\sigma}) + H.C. \right] + H_{imp.}$$

- **Eigen energy E_k (neglect t' and H_{imp}):** $E_k =$

$$\pm t \left[1 + 4\cos(\frac{\sqrt{3}a}{2} k_x)\cos(\frac{3a}{2} k_y) + 4\cos^2(\frac{\sqrt{3}a}{2} k_x) \right]^{1/2}$$

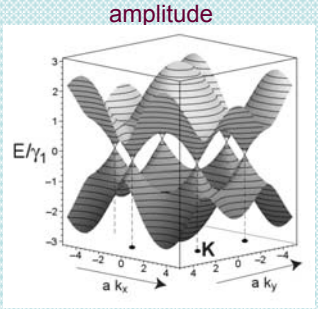

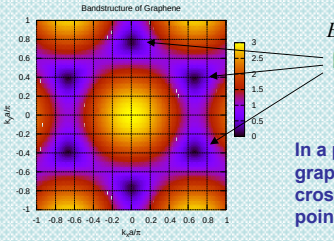

$E(\vec{q} = \vec{K}) = 0$

Dirac points

In a perfect graphene sheet μ crosses the Dirac points

Dispersion relation near Dirac point

- Low energy Hamiltonian : expand around the Dirac point

K→K1+k (K1 is one of the 6 Dirac points or vertices)

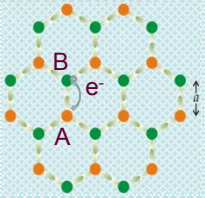

- Dirac's (relativistic) equation with zero mass

$$\mathrm{H} = \hbar \upsilon_F \vec{\sigma} \cdot \vec{k} = \hbar \upsilon_F \begin{pmatrix} 0 & k_x - ik_y \\ k_x + ik_y & 0 \end{pmatrix}, \quad \mathrm{H} \begin{pmatrix} \psi_A \\ \psi_B \end{pmatrix} = E \begin{pmatrix} \psi_A \\ \psi_B \end{pmatrix}$$

Pauli "spin" matrices

"Pseudospin" state

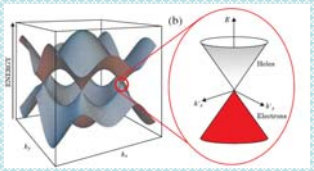

$$E(\vec{k}) = \pm \upsilon_F \hbar |\vec{k}|, \quad \upsilon_F \approx 10^6 ms^{-1}$$

Massless quasiparticle !

- Well-defined chirality: σ·p = +1 or -1:

Positive for electron and negative for hole (positron)

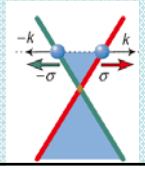

Preparation of Single-Atomic Layer Graphite – Mission Impossible ?

Andre Geim
51
Univ. Manchester

Konstantin Novoselov
36
Univ. Manchester

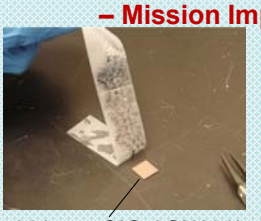

290 nm SiO_2/ Si(100)

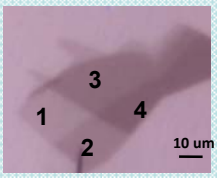

Seeing a single-atomic layer graphene !

Graphite **Tape** **Optical Micro.**

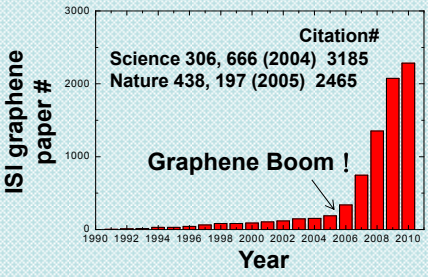

Geim and Novoselov: 2010 Nobel Prize in Physics

{ a perfect 2D crystal does exist
High tech. in not the only route

Superior Material Properties in Graphene ⋮

Practical application in the future

- Extremely light weight，density~0.77 mg/m² 。
- Tensile strength 100 times higher than steel 。
- Nearly Transparent，light adsorption ~ 2.3% 。
- Conductivity 1.6 times higher than copper 。
- Fast electron traveling speed ~ c/300 。
- At RT，thermal conductivity 10 times higher than copper 。

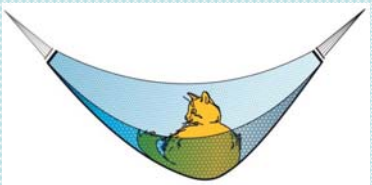

A hanger made by 1m² graphene(~0.77mg and invisible) : hold up to 4kg without breaking 。

Touch Panel

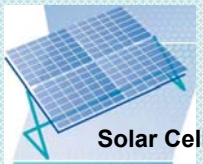

Solar Cell

Nano electr.
Flexible Electr.

⋮

Future Applications of Graphene
Graphene can be used as flexible and stretchable transparent electrodes in the future.

Fabrication of large area graphene

Chemical Vapor Deposition
SiC high Temp. anneal } Succeeded in producing graphene roll with 70 cm in width

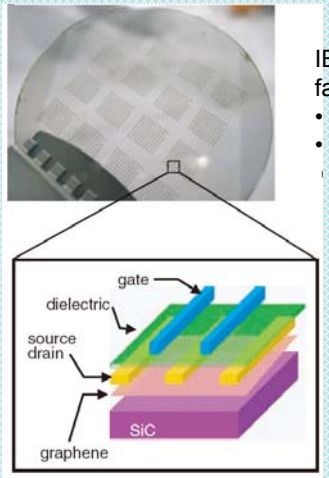

IBM team demonstrated wafer-sized fabrication of graphene transistor array
- Cut-off freq. for current gain:100 GHz.
- Cut-off freq. for power gain:10 GHz.

Few-layer graphene has great potential in replacing the silicon based electronics.

Angle-resolved photoemission spectroscopy (ARPES)

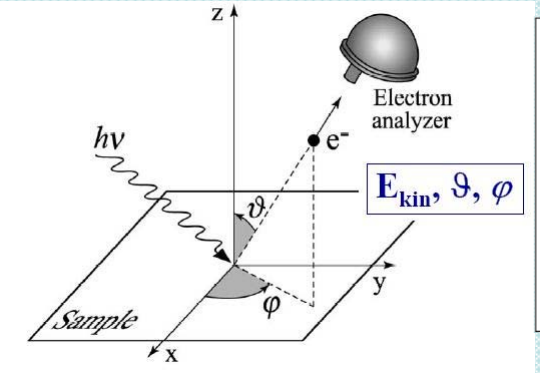

$$\mathbf{K} = \mathbf{p}/\hbar = \sqrt{2mE_{kin}}/\hbar$$

$$K_x = \frac{1}{\hbar}\sqrt{2mE_{kin}}\sin\vartheta\cos\varphi$$

$$K_y = \frac{1}{\hbar}\sqrt{2mE_{kin}}\sin\vartheta\sin\varphi$$

$$K_z = \frac{1}{\hbar}\sqrt{2mE_{kin}}\cos\vartheta$$

- **E_{kin}, K can be measured in UHV**
- **Conservation law : $E_{kin}=h\nu - \varphi - E_B$**
  $k_f - k_i = k_v$
- **E_B and k in solid can be determined**
  ⇨ direct probe for dispersion relation in solids

Angle-resolved photoemission spectroscopy (ARPES)

- State-of-art apparatus :
  2meV energy resolution and 0.2 degree angular resolution
- Surface sensitive : only surface electrons carry inherent information without suffering complicated scattering

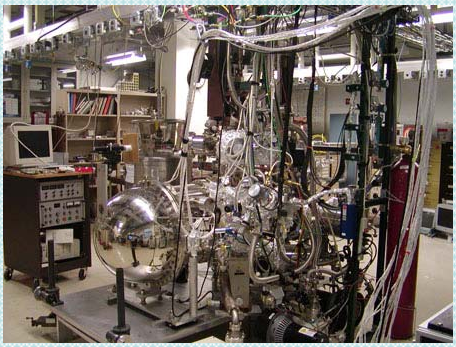

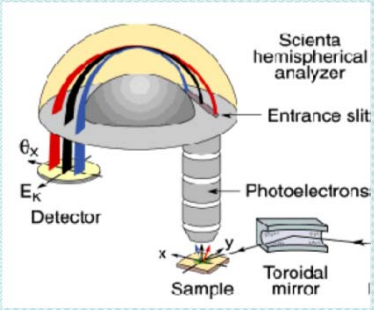

ARPES at Shen's group at Stanford Univ.

Direct observation of Dirac Fermions

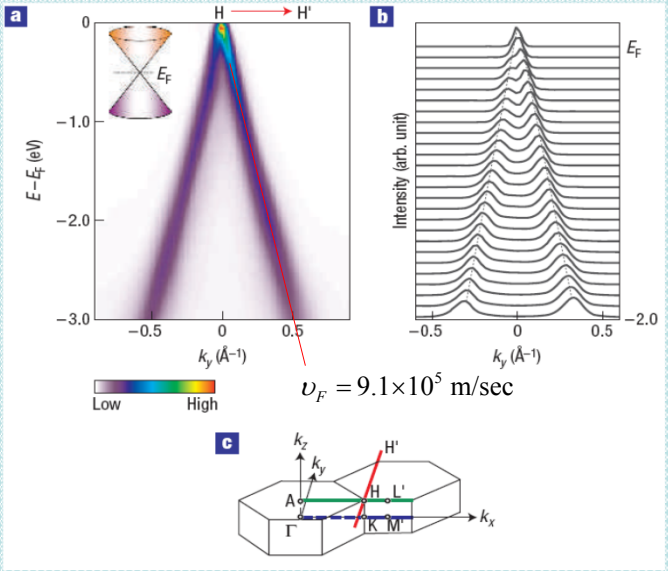

$$\upsilon_F = 9.1\times10^5 \text{ m/sec}$$

M. I. Katnelson, K. S. Novoselov, and A. K. Geim, cond-mat/0604323

Relativistic Physics in Condensed Matter System-

Klein Paradox in Graphene

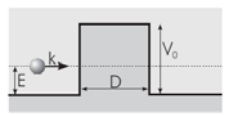

Klein paradox: unimpeded penetration of relativistic particles through high and wide potential barriers - 1930

Monolayer **Bilayer**

Barrier *always* transparent for angles close to normal incidence !!

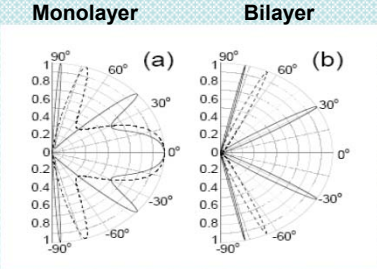

Massive fermions are reflected close to normal incidence!

Impurity scattering in the bulk of graphene is strongly suppressed !!!

Fabry-Pérot (FP) Interference in p-n-p Heterojunctions

- Shytov, et al., PRL 08'

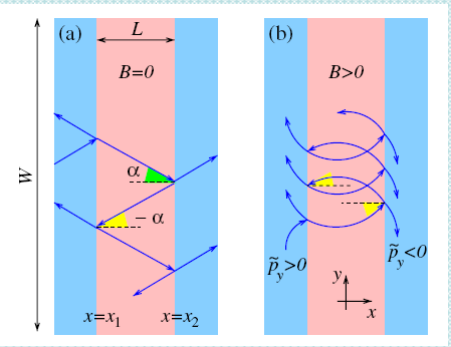

p-n-p junctions

Interference due to e⁻ bouncing b/w p-n interfaces

- **FP interference :**

$$\Delta\theta = 2\theta_{WKB} + \Delta\theta_1 + \Delta\theta_2,$$

$$\theta_{WKB} \equiv \int_1^2 p_x(x')dx',$$

$\Delta\theta_{1(2)}$: Klein Backreflection phase change.

- **Conductance oscillation in the p-n-p junctions**

$$G_{osc} \sim \cos(\Delta\theta)$$

- **($\Delta\theta_1$+ $\Delta\theta_2$) do not cancel at finite field.**

- **For a perfect Transmission (T = 1) at normal incident (α=0) suggested by Klein paradox, the back-reflection phase should undergo a π-shift at α=0 !**

Quantum Interference in Graphene p-n Heterojunctions

- Young, et al., Nat. Phys. 09'

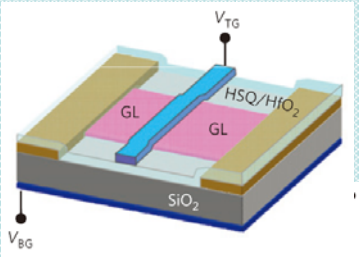

- Tuning α across 0 by B field
- Phase shift at field B ~ 400mT
- Perfect transmission at normal incident → Klein Paradox !

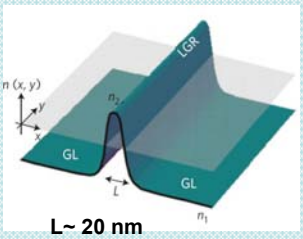

L~ 20 nm

p-n junction : (n1*n2)<0

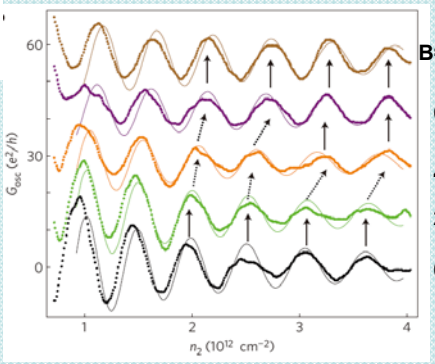

B=800 mT
600 mT
400 mT
200 mT
0 mT

Transport in Graphene

Novoselov, et al., Science 04', Nature 05'

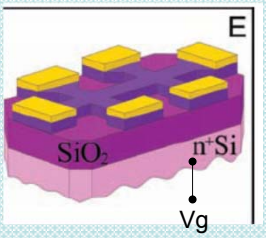

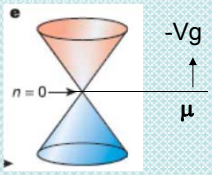

- Chemical potential tuned by V_g~ n_c
- Ambi-polar field effect
- Robust minimal conductivity ?

  $\sigma_{min} = 4e^2/h$, at Dirac point

Electric field effect in graphene

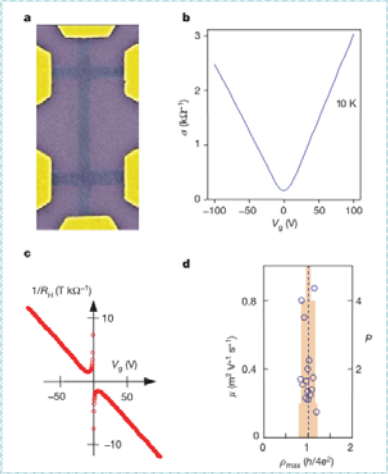

Integer QHE in Graphene

Novoselov, et al., Nat. Phy. 06'

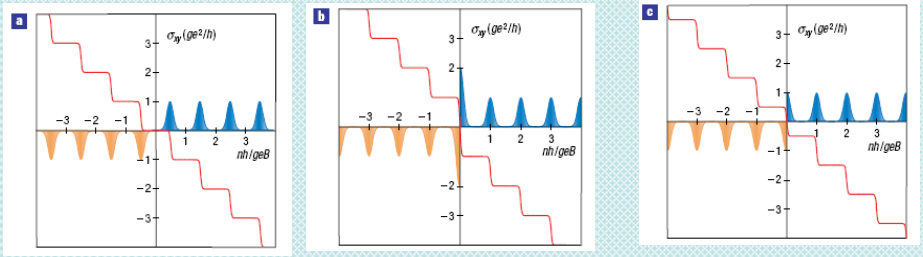

2-DEG
free-Fermion

Bilayer graphene
Berry's phase 2π

Single-layer graphene
Berry's Phase π

- For a given B, D.O.S. at each Landau level = gB/Φ_0
- Anomaly at lowest Landau level in graphene
- Internal field (Berry's phase) ⇨ non-zero QHE in zero external field*

* Haldane, et al., PRL 88'

Massless Dirac Fermion and π Berry's phase

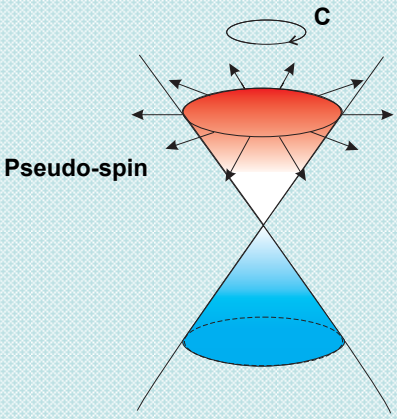

- Pseudospin eigenstate along $\vec{k}$
- Closed contour C in k space associated with cycltron path
- Berry's phase acquired along path C

$$\gamma(C) = -\iint_C \boldsymbol{\Omega}\cdot d\vec{S} = -\frac{1}{2}\Omega(C) = -\pi$$

Solid angle

Parallel transport of vector v on curved surface

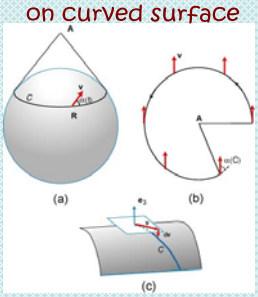

Quantum Hall Effect at Room Temperature !

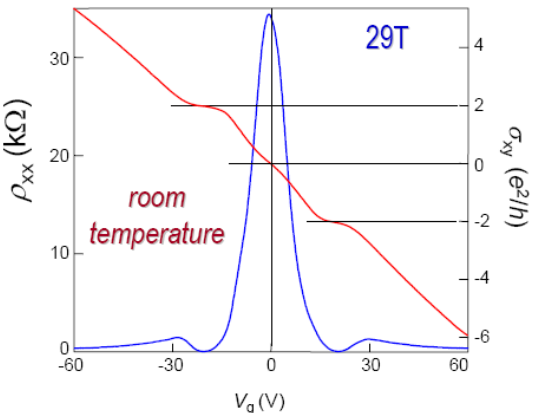

$$E_n = sign(n)(2n)^{1/2}\frac{\hbar \upsilon_F}{\ell_B}$$

For $B = 29$ Tesla, $E_1 - E_0 = 0.196\text{eV} = 2271\text{K}$!!

$$cf: \quad E_n = (n+\frac{1}{2})\hbar\omega_C, \ \Delta E = \hbar\omega_C = 3.36meV = 39K$$

Characterization of the thickness: Atomic Force Microscope

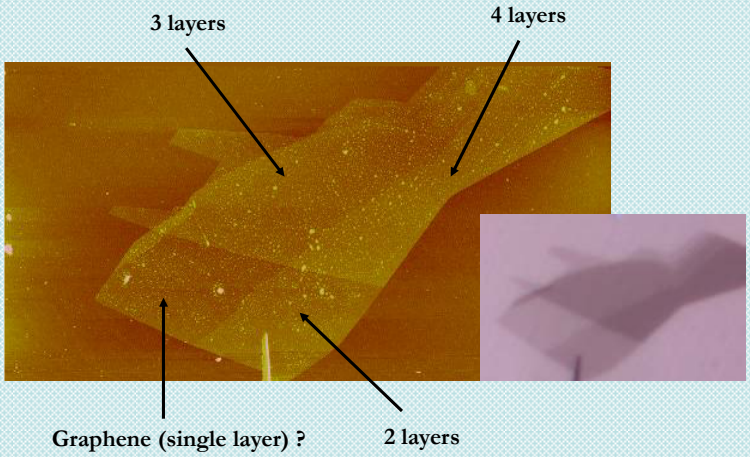

Measured thickness ~ 0.8 nm > 0.34 nm

Characterization of thickness: Raman spectroscopy

Single and sharp 2D peak in Single-layer graphene !!

Double Resonant Raman Process
- Ferrari, et al., PRL 06

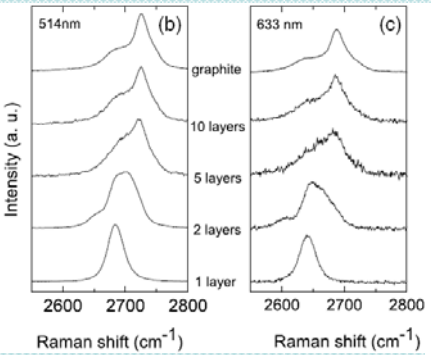

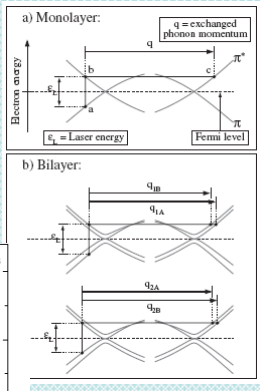

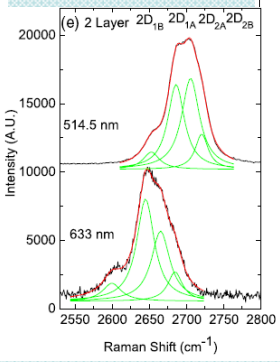

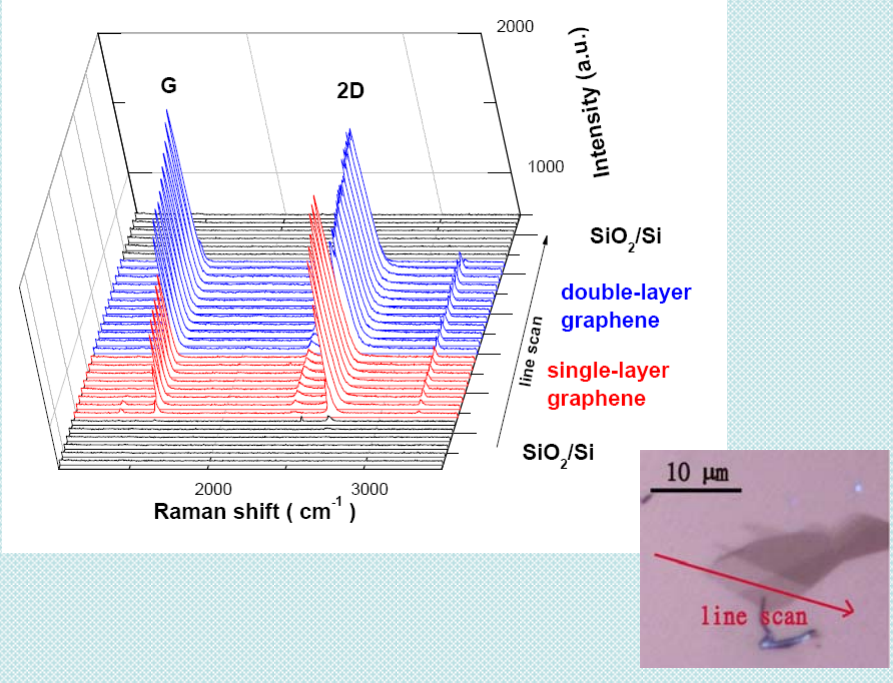

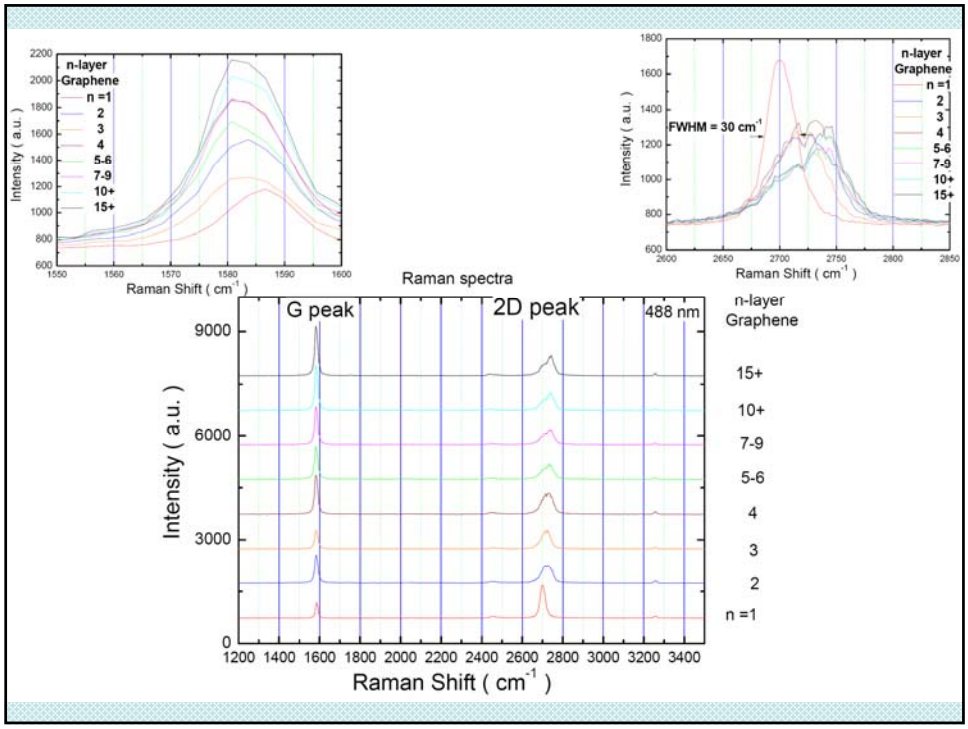

Raman Spectroscopy

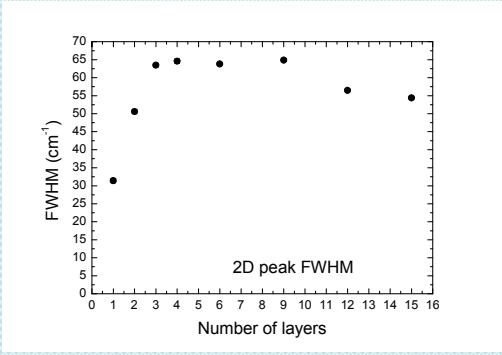

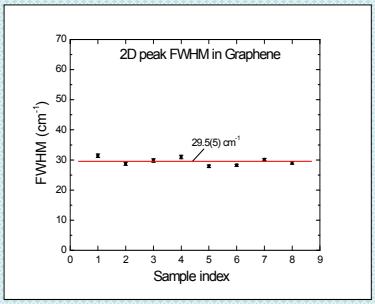

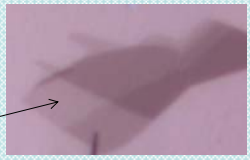

Single-layer graphene !!

Large Area Graphene Fabrication- CVD on Cu

-- Li, et. al., Science 09'

Self-limiting growth of graphene on copper

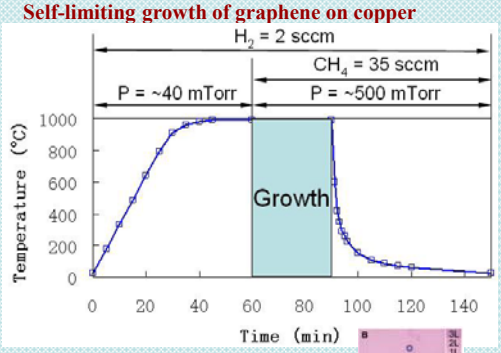

Bilayer graphene ~ 3-4%
Trilayer or thicker < 1%
Single atomic layer graphene >95%

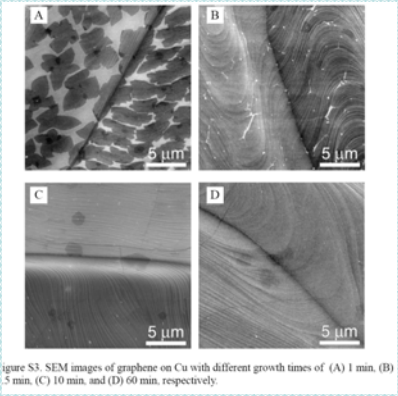

igure S3. SEM images of graphene on Cu with different growth times of (A) 1 min, (B) 5 min, (C) 10 min, and (D) 60 min, respectively.

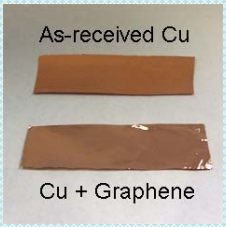

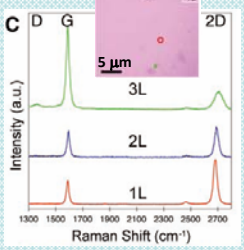

Large Area Graphene Fabrication-CVD on Cu

-- Li, et. al., Science 09'

Self-limiting growth of graphene on copper

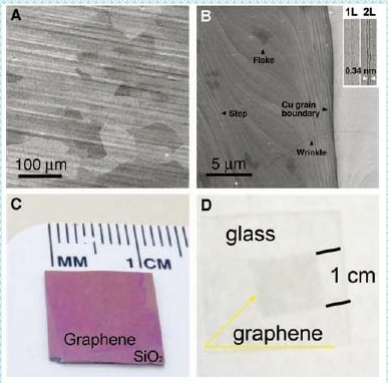

Mobility ~ 4000 cm²/V-sec

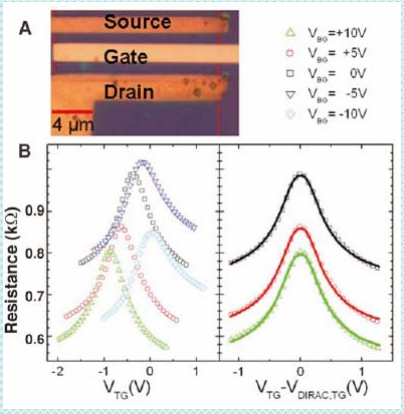

Large Area Graphene Fabrication- SiC

-- Berger, et. al., J. Phys. Chem. B 04′

Thermal decomposition at the surface of SiC(0001):

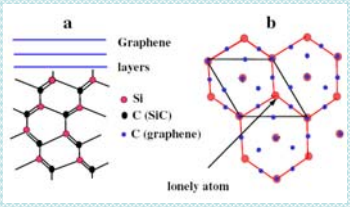

Sublimation of Si
+
graphitize the excess C

Thickness can be controlled by Temp.

4H-SiC (Si terminated)

6H-SiC (C terminated)

TABLE 1: Sample Properties[a]

Sample	C:Si	Thickness	R_{sq}	Mobility
A	10	3 ML	1.5 kΩ	1100 cm²/Vs
B	∞	>5	2.2	
C	9	3	22	
D	10	3	33	15
E	9	3	225	
F	7	2.5		

[a] Ratio of intensities in the C(271 eV) and Si(92 eV) AES peaks, calculated thickness in graphene monolayers, square resistance at 4 K, and mobility (where measured).

LEED image

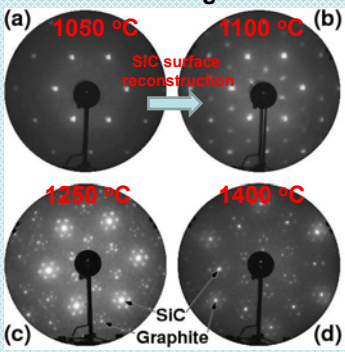

STM image

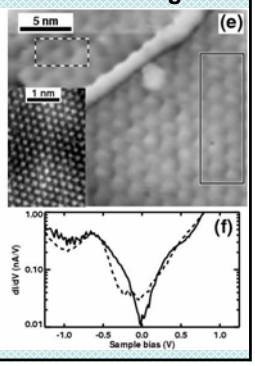

Large Area Graphene Fabrication- MBE

-- Park, et. al., Adv. Mater. 10′

Epitaxial Graphene using Molecular Beam Epitaxy

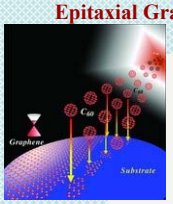

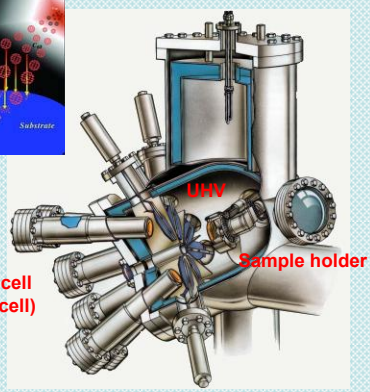

Effussion cell
(Knudsen cell)

Raman Spectrum

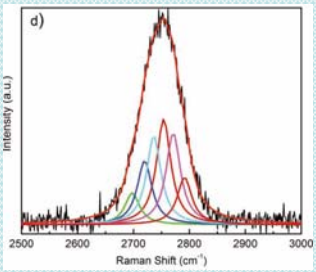

Trilayer graphene

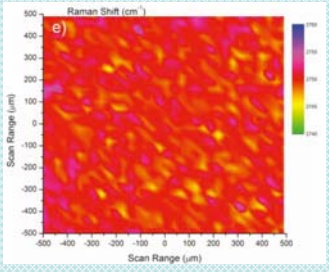

- C_{60} and graphite filament source
- Filament source at 1200°C
- Substrate temp. @ 1400°C
- Thickness control by carbon flux and substrate temp.

Can Graphene-based device replace current silicon based device ?

Comparison between graphene and semiconductor

	Semiconductor	Graphene
Electronic structure	Band gap > 1 eV	No-band gap (linear dispersion)
carrier	massive	massless (speed: c/300)
chirality	No	Yes
Dimensionality	Quasi-2D via electric field confinement (t~5-50 nm)	Ideal 2D (t ~ 0.34 nm)

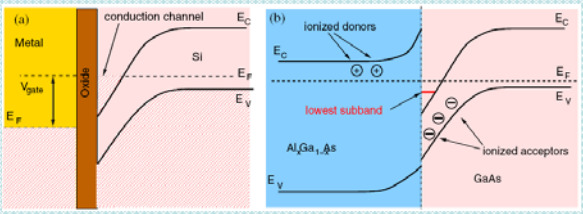

Quasi two-dimensional subband at interface

Graphene Nano-ribbon : Energy Gap Engineering

• **Gap opening due to quasi-1D confinement of the carriers**

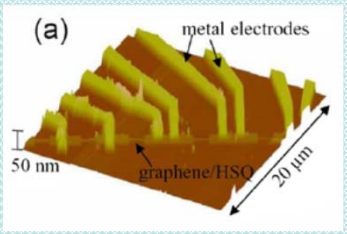

$$E_g = \frac{\alpha}{(W - W^*)}$$

$$\alpha \sim 0.2 eV \cdot nm, W^* = 16 nm$$

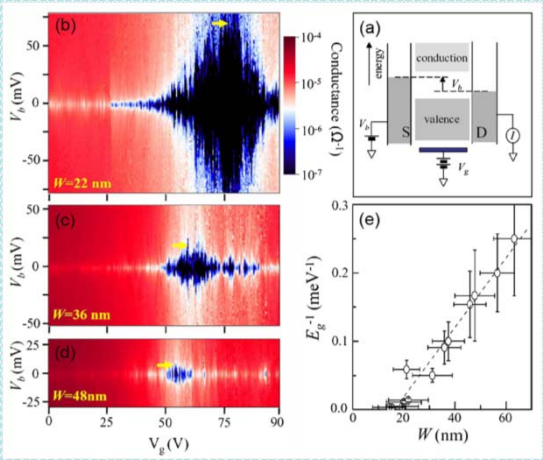

Field effect device: replacing current silicon-based device

- **Full-electric field tuning of band gap in bilayer graphene(BLG)**

-- Zhang *et al.*, Nature 09'

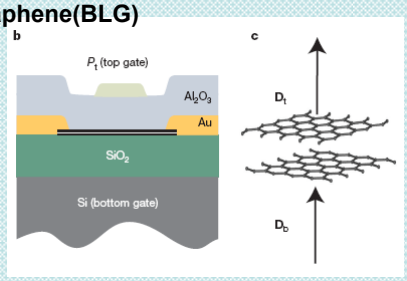

$$\vec{D} = [\varepsilon_b(V_{bg} - V_{bg0})/d_b - \varepsilon_t(V_{tg} - V_{tg0})/d_t]/2$$

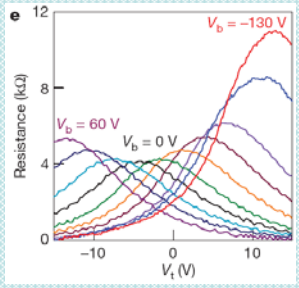

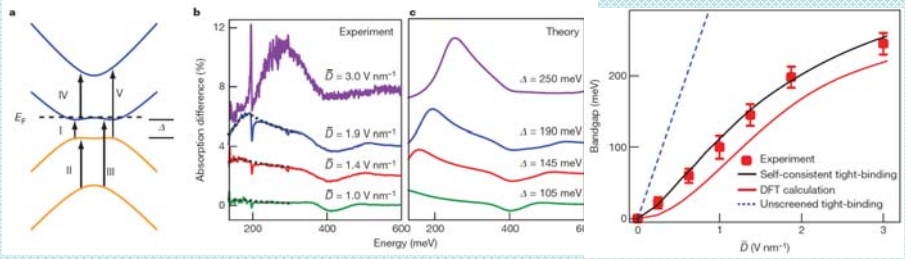

SQUID device

S/Graphene/S Josephson Junction

Heersche, et al., Nature 07'

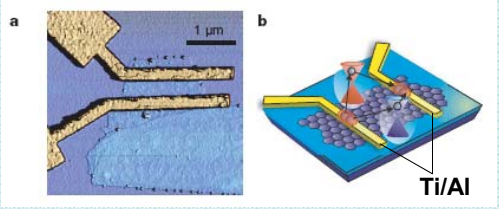

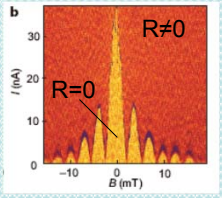

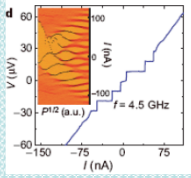

Shapiro steps

- **S electrodes spaced by graphene**
- **DC and AC Josephson effect**
- **Phase coherent transport at Dirac point**

DC Josephson :

$$I_C \propto \frac{\sin(\pi\Phi/\Phi_0)}{\pi\Phi/\Phi_0},\ \Phi = \text{total magnetic flux}$$

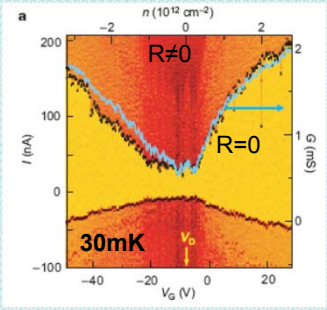

Spin electronics:

Spin transport and precession in graphene at room temperature

- Tombros et al., Nature 07'

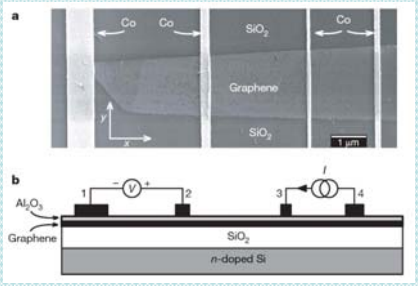

- **Large spin emf signal at R.T.**
- **Spin diffusion length λ_{sf}~ 1.5-2 μm**
- **Spin relaxation time τ_{sf} ~ 100ps**

$$R_{non-local} \propto \int_0^\infty P(t)\cos(\omega_L t)\exp(-t/\tau_{sf})dt$$

cf : λ_{sf}~ 0.5 μm

τ_{sf} ~ 10 ps in copper

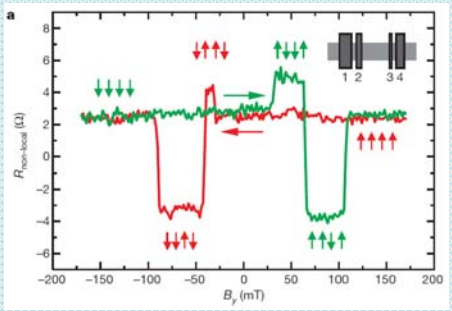

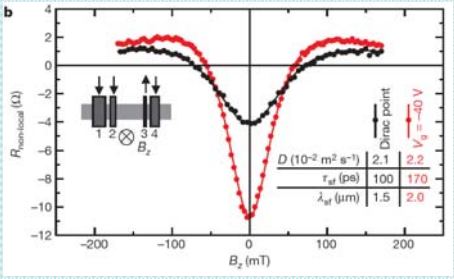

Optical application

- **Graphene photoluminescence(PL)**

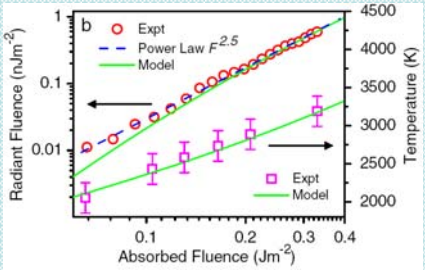

- **Ultrafast photon excitation ~ 30 fs: carriers with transient T > 2000K**
- **PL: thermal emission visible spectra range (1.7 – 3.5 eV) bigger than excitation laser ~ 1.5 eV**

- **PL in graphene oxide (GO) and gapped (bilayer) graphene:**

1L : single-layer graphene after O2 plasma treatment

PL intensity

Layer contrast

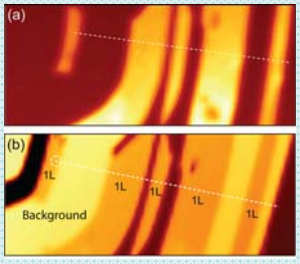

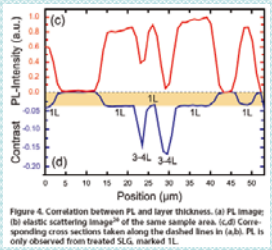

Figure 4. Correlation between PL and layer thickness. (a) PL image; (b) elastic scattering image[26] of the same sample area. (c,d) Corresponding cross sections taken along the dashed lines in (a,b). PL is only observed from treated SLG, marked 1L.

Graphene Nanophotonics

- F. Javier Garcia de Abajo, Science 13'

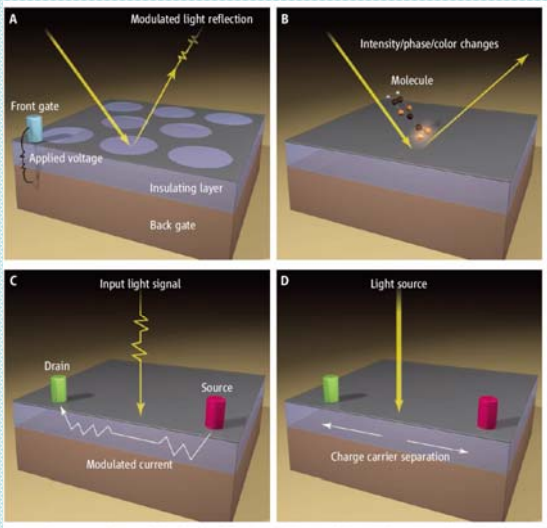

The graphene nanophotonics landscape. (**A**) Light modulation of the optical response of graphene is realized by applying voltages through electrical gates (*4*–*6*). (**B**) Molecular detection is accomplished through the modifications in the optical response associated with changes in the concentration of charge carriers (*9*). (**C**) Measurement of the electrical current modulated by photon absorption leads to efficient light detection (*11*, *12*). (**D**) Light harvesting occurs when the energy of absorbed photons is converted into charge carriers that are separated by doped gates to generate a net current.

RESEARCH FUNDING

Europe's €2 Billion Bet on the Future

This month, the European Union will pick two futuristic research proposals and shower them with up to €1 billion each. But will it be money well spent?

Science Magazine

E.U. Flagships: The Candidates at a Glance

FuturICT. Proposes massive data mining to build a planetary scale simulator freely available for use. Promises "historic breakthroughs" in "revealing the hidden laws and processes underlying societies." 1

<< **Graphene.** Better batteries, lighter planes, and flexible electronics are some of graphene's promises. "Disruptive science" is hard to do piecemeal, proponents say; a Flagship grant would allow for coordination. 2

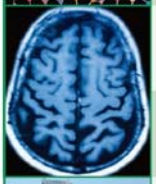

Guardian Angels. A network of energy-harvesting sensors that can monitor people's health status, scan the environment for dangers, and provide advice "to increase the happiness people experience." 3

<< **The Human Brain Project.** Supercomputers would simulate and help people understand the human brain. Key argument: Only a model can bring together everything we know about neuroscience. 4

IT Future of Medicine. Aims to use individual medical data to build a personalized computer model for 500 million Europeans. The approach is currently pioneered in cancer treatment. 5

<< **RoboCom.** Inspired by animals, its goal is to develop "robot companions" better able to respond to human needs. Engineering these machines would also help understand the design principles of biological bodies and brains. 6

A Long Game for Carbon-Based Materials

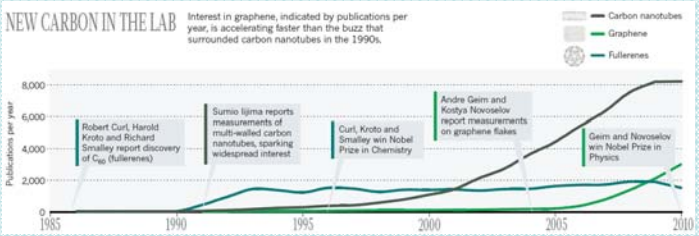

"It typically takes any technology some 20 years to emerge from the lab and be commercialized."

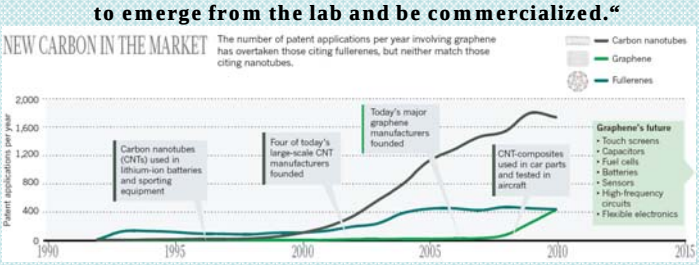

We are observing a revolution in electronics industry !
Commercial product made of graphene will have its debut in our time.

"Graphene will have its place, but it will just take longer than people think."

Cutting cost
+
higher quality

Graphene manufacturers

BGT BLUESTONE GLOBAL TECH
GRAPHENE INDUSTRIES
XG sciences
Vorbeck Materials
ANGSTRON MATERIALS
GRAPHENE SUPERMARKET
CVD
DGS
⋮

PartII: Concluding Remarks

- **Massless Dirac Fermion and insensitive to impurity scattering**
- **Marginal Fermi-liquid behaviour**
- **Unavoidable defects and disorder in 2-D graphene**
- **Exhibit robust minimal conductivity and shifted IQHE**
- **Phase coherent transport at the Dirac point**
- **Appearance of band gap in graphene nanoribbon**

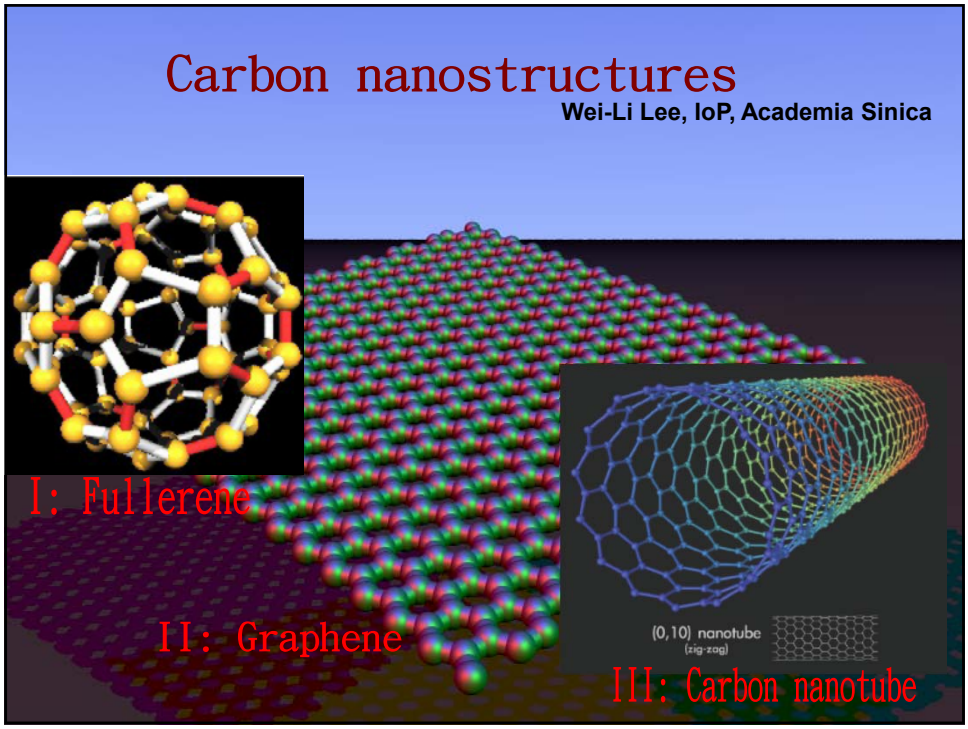

Part III

Carbon nanotube

Outline
- Structure of carbon nanotube
- Fabrication of carbon nanotube
- electronic property in carbon nanotube
- Applications of carbon nanotube

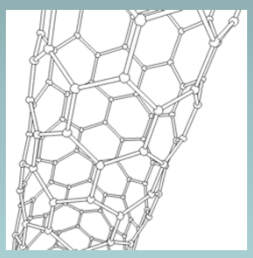

semiconducting

Zigzag (8,0) carbon nanotub

Structure of single wall carbon nanotube

Rolling of a 2-D graphene sheet

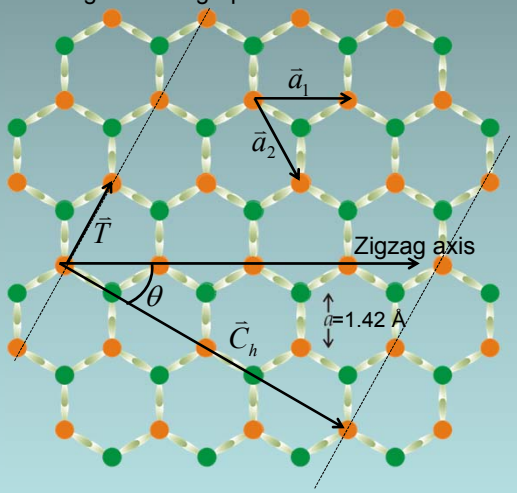

Chiral (Circumferential) vector

$$\vec{C}_h \equiv n\vec{a}_1 + m\vec{a}_2$$

Translational vector

$$\vec{T} \perp \vec{C}_h$$

Tube diameter d_t

$$d_t = \left|\vec{C}_h\right| / \pi$$

$$= \frac{a}{\pi}\sqrt{3(m^2 + mn + n^2)}$$

Angle $\theta = \tan^{-1}[\sqrt{3}m/(m+2n)]$

Rolling of a 2-D graphene sheet

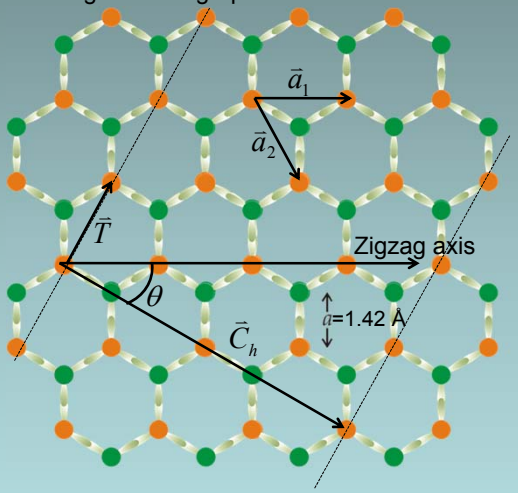

Label a carbon nanotube

(n, m),

where $\vec{C}_h \equiv n\vec{a}_1 + m\vec{a}_2$

or

(d_t, θ)

Tube diameter

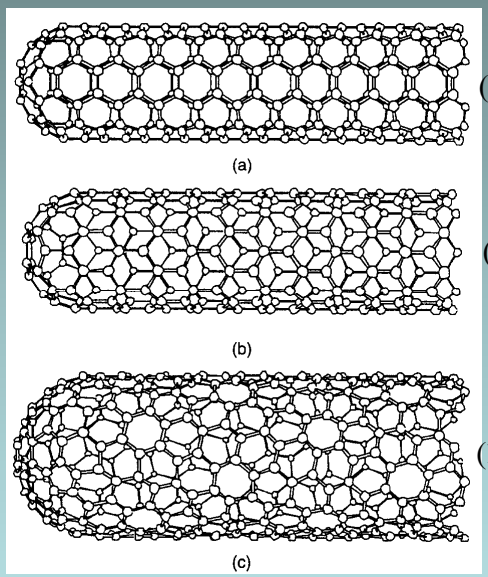

Armchair (5,5) (n,n)

Zigzag (9,0) $(n,0)$

Chiral (10,5) (n,m)

Electronic Band Structure in Materials

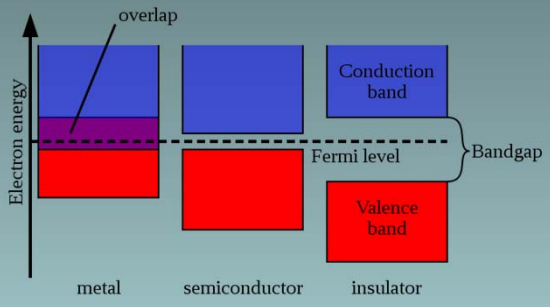

Armchair tubes are all metallic !!

Rule : metallic for n-m = 3 q
(q: an integer)

Why ?

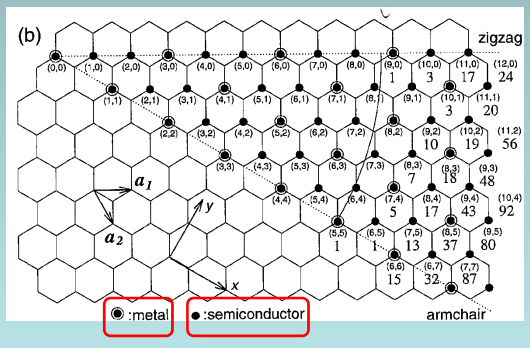

Fabrication of carbon nanotube

(I) Laser evaporation

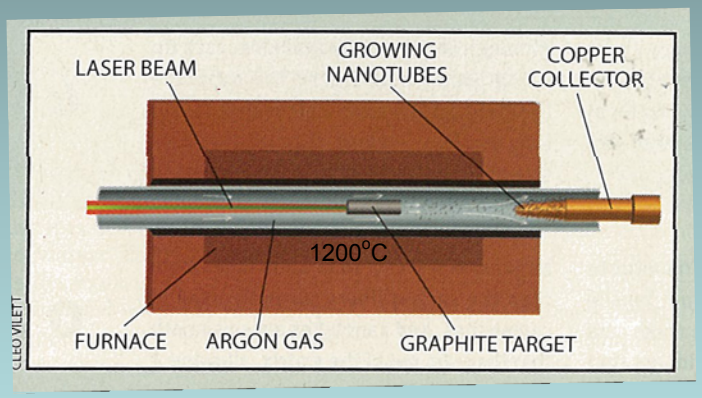

(II) Carbon arc discharging:

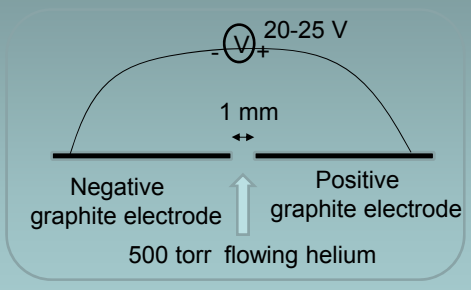

- Nanotubes (NTs) will form on the negative electrode : mostly multi-walled NTs
- Incorporate Co, Ni, Fe catalysts in the positive electrode : Single-walled NTs

(III) Plasma enhanced Chemical vapor deposition (CVD)

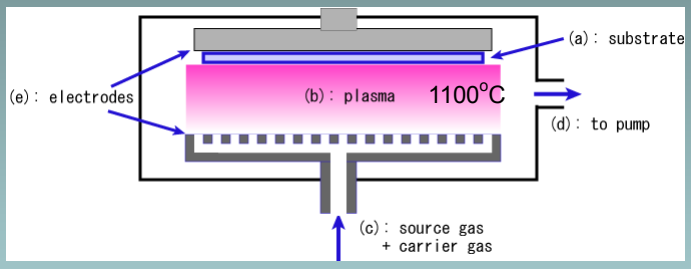

(a) Substrate : a thin layer of metal catalyst particles, Co, Ni, Fe..etc
(b) Source gas : a carbon-containing gas, CH_4, C_2H_2 …etc
Carrier gas : H_2, N_2 …etc
(c) Nanotube forms along the field direction
(d) Favorable for large scale production

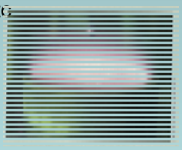

Growth mechanism of carbon nanotube

(I) Not well-understood !
(II) Absorption of monomer C, dimer C_2, trimer C_3
(III) Scootter mechanism for the metal particles served as catalyst

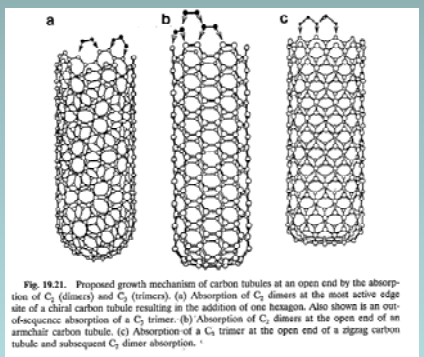

Fig. 19.21. Proposed growth mechanism of carbon tubules at an open end by the absorption of C_1 (dimers) and C_3 (trimers). (a) Absorption of C_3 dimers at the most active edge site of a chiral carbon tubule resulting in the addition of one hexagon. Also shown is an out-of-sequence absorption of a C_3 trimer. (b) Absorption of C_2 dimers at the open end of an armchair carbon tubule. (c) Absorption of a C_3 trimer at the open end of a zigzag carbon tubule and subsequent C_2 dimer absorption.

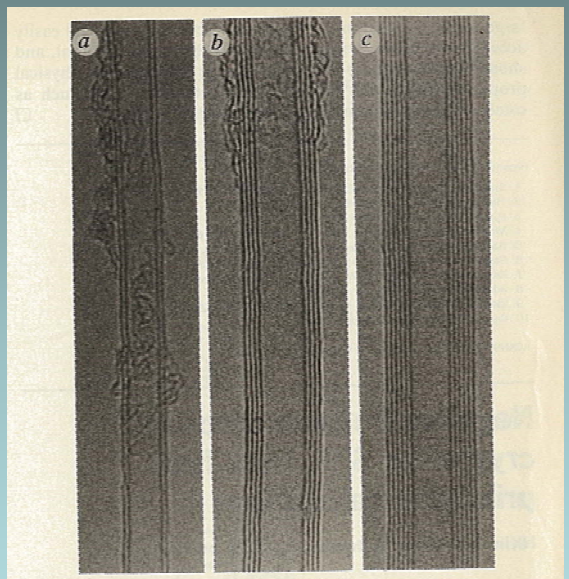

FIG. 3 High-resolution electron micrographs of typical tubes present in samples prepared under helium at 500 torr as described in the text. The number of layers ranges from two to many. The distance between consecutive carbon layers in the tubes is 0.34 nm.

Multi-Walled NTs (MWNTs):

Inter-layer distance ~0.34 nm

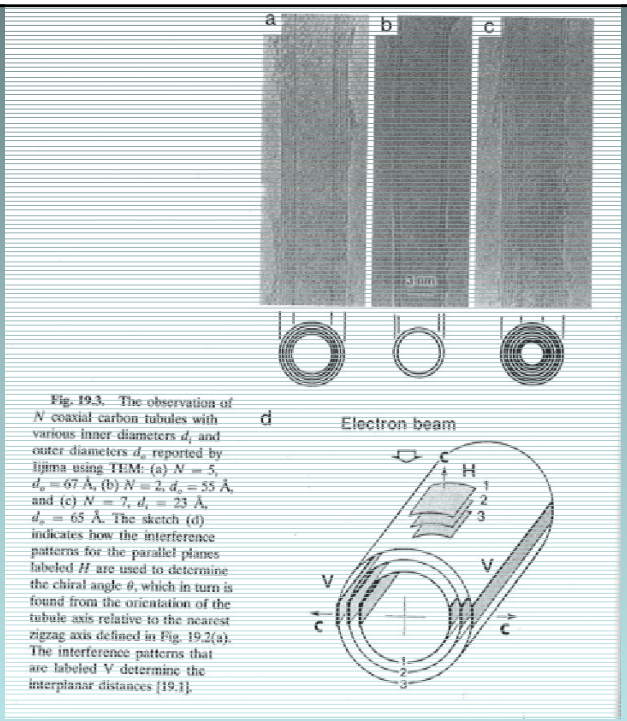

Fig. 19.3. The observation of N coaxial carbon tubules with various inner diameters d_i and outer diameters d_o reported by Iijima using TEM: (a) $N = 5$, $d_o = 67$ Å, (b) $N = 2$, $d_o = 55$ Å, and (c) $N = 7$, $d_i = 23$ Å, $d_o = 65$ Å. The sketch (d) indicates how the interference patterns for the parallel planes labeled H are used to determine the chiral angle θ, which in turn is found from the orientation of the tubule axis relative to the nearest zigzag axis defined in Fig. 19.2(a). The interference patterns that are labeled V determine the interplanar distances [19.1].

MWNTs :

Coaxially stacked cylinders

Not Scroll-like tubes !

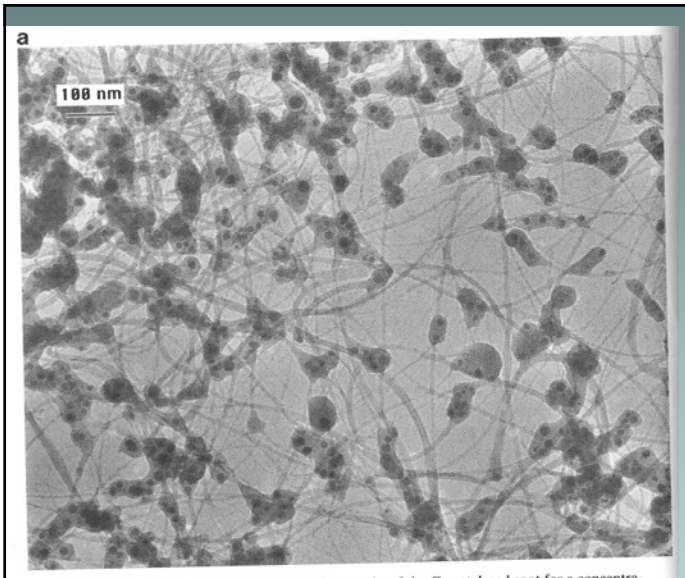

Fig. 19.6. (a) Transmission electron micrographs of the Co-catalyzed soot for a concentration of 4% Co. The threads in the figure are apparently individual nanotubules or bundles of nanotubes such as shown in (b). Most of the as-prepared nanotubes are covered with carbon soot [19.31].

Single-Walled NTs (SWNT

Co catalyst particles found at the ends of the tubes

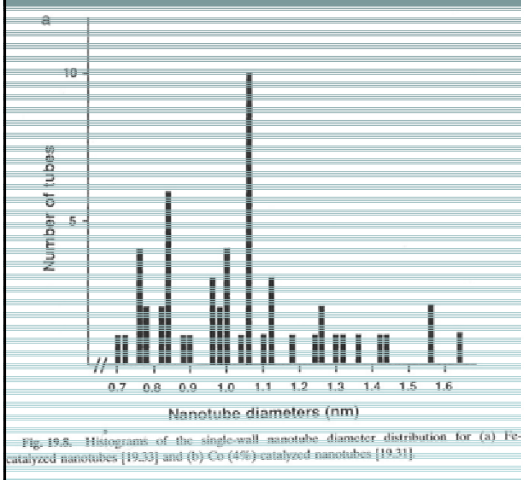

Fig. 19.8. Histograms of the single-wall nanotube diameter distribution for (a) Fe-catalyzed nanotubes [19.33] and (b) Co (4%)-catalyzed nanotubes [19.31].

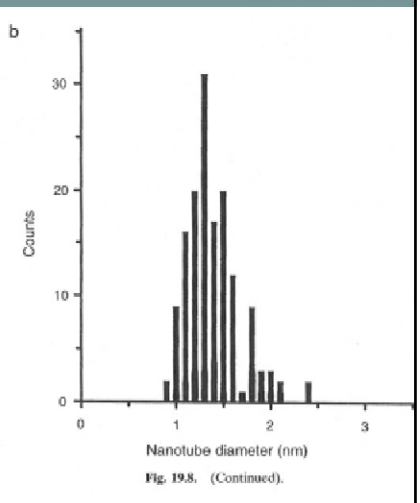

Fig. 19.8. (Continued).

Type of catalyst can result in different SWNTs size distribution

"Breathing" modes of carbon nanotube

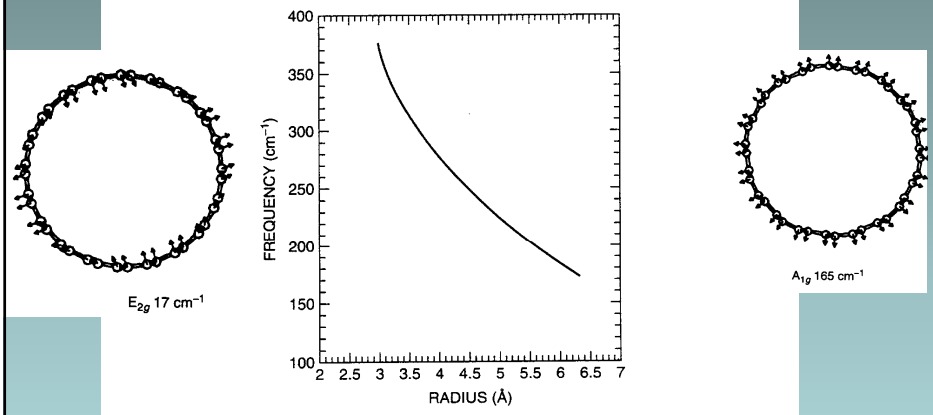

Figure 5.20. Plot of the frequency of the Raman A_{1g} vibrational normal mode versus the radius of the nanotube. (10 Å = 1 nm). (Adapted from R. Saito, G. Dresselhaus, and M. S. Dresselhaus, *Physical Properties of Nanotubes*, Imperial College Press, 1998.)

SWNT stiffness is larger for smaller tube : higher elastic (strain) energy
Alternative way to determine the SWNT diameter d_t

Electronic property of carbon nanotube

Rolling of a 2-D graphene sheet

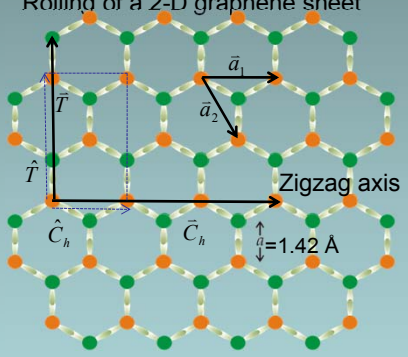

$$|\vec{a}_1| = |\vec{a}_2| \equiv a_0 = \sqrt{3} \times a_{cc}$$

Lattice vector for a 1-D CNT (n,m):

$$\hat{C}_h = \frac{a_0}{2d_R}(\sqrt{3}(n+m),(n-m)),$$

$$\hat{T} = \frac{\sqrt{3}a_0}{2d_R}(-(n-m),\sqrt{3}(n+m))$$

$$d_R = \begin{cases} 3d & \text{if (n - m) is a multiple of 3d} \\ d & \text{otherwise} \end{cases}$$

, where d is the highest common divisor of (n,m

example: For (3,0) , d_R = 3

Reciprocal lattice vector for a 1-D CNT (n,m):

$$\vec{b}_1 = \frac{2\pi}{Na_0}(\sqrt{3}(n+m),(n-m)),$$

$$\vec{b}_2 = \frac{2\pi}{\sqrt{3}Na_0}(-(n-m),\sqrt{3}(n+m))$$

$$R_i \cdot b_j = 2\pi\delta_{ij}$$

$$N \equiv \frac{2(m^2+n^2+nm)}{d_R}, \quad \#\text{ of hexagons per } \hat{T}.$$

Table 19.2

Values for characterization parameters[a] for selected carbon nanotubes labeled by (n,m) [19.5, 82].

(n,m)	d	d_R	d_t (Å)	L/a_0	T/a_0	N	$\psi/2\pi$	τ/a_0	Ω/d
(4, 2)	2	2	4.14	5	$\sqrt{21}$	28	5/28	$\sqrt{21}/14$	5
(5, 5)	5	15	6.78	$\sqrt{75}$	1	10	1/10	1/2	1
(9, 0)	9	9	7.05	9	$\sqrt{3}$	18	−1/18	$\sqrt{3}/2$	−1
(6, 5)	1	1	7.47	$\sqrt{91}$	$\sqrt{273}$	182	149/182	$\sqrt{3/364}$	149
(7, 4)	1	3	7.55	$\sqrt{93}$	$\sqrt{31}$	62	17/62	$1/\sqrt{124}$	17
(8, 3)	1	1	7.72	$\sqrt{97}$	$\sqrt{291}$	194	71/194	$\sqrt{3/388}$	71
(10, 0)	10	10	7.83	10	$\sqrt{3}$	20	−1/20	$\sqrt{3}/2$	−1
(6, 6)	6	18	8.14	$\sqrt{108}$	1	12	1/12	1/2	1
(10, 5)	5	5	10.36	$\sqrt{175}$	$\sqrt{21}$	70	1/14	$\sqrt{3/28}$	5
(20, 5)	5	15	17.95	$\sqrt{525}$	$\sqrt{7}$	70	3/70	$1/(\sqrt{28})$	3
(30, 15)	15	15	31.09	$\sqrt{1575}$	$\sqrt{21}$	210	1/42	$\sqrt{3}/28$	5
⋮	⋮	⋮	⋮	⋮	⋮	⋮	⋮	⋮	⋮
(n,n)	n	$3n$	$\sqrt{3}na/\pi$	$\sqrt{3}n$	1	$2n$	$1/2n$	1/2	1
$(n,0)$	n	n	na/π	n	$\sqrt{3}$	$2n$	$-1/2n$	$\sqrt{3}/2$	−1

[a] Ω is given by Eq. (19.13); T is given by Eq. (19.7) with $a_0 = \sqrt{3}a_{c-c}$; L is the length of the chiral vector nd, given by Eq. (19.2); N is given by Eq. (19.9); ψ is given by Eq. (19.12); τ is given by Eq. (19.11); Ω/d is the number of complete 2π revolutions about the tubule axis to reach a lattice point.

1-D Band structure for an armchair CNT (N_y,N_y):

2-D graphene sheet

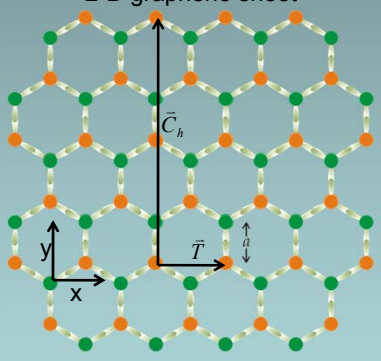

- Dispersion relation for 2D graphene :

$$E^{2D}(k_x,k_y) = \pm t[1+4\cos(\frac{\sqrt{3}a}{2}k_x)\cos(\frac{3a}{2}k_y)+4\cos^2(\frac{\sqrt{3}a}{2}k_x)]^{1/2} \quad \text{Eq(1)}$$

Bohr-Sommerfeld quantization rule:

$$\int_{path}^{closed} p\cdot d\ell = qh\,,\ \text{q is integer number}$$

- In 1D armchair CNT :

  k_y satisfy periodic boundary condition

$$\because k_y 3aN_y = 2\pi q$$

$$\therefore E^{1D}{}_{arm}(k_x = k)$$

$$= \sum_{q=1}^{N_y} \pm t[1 \pm 4\cos(\frac{\sqrt{3}a}{2}k)\cos(\frac{\pi q}{N_y})+4\cos^2(\frac{\sqrt{3}a}{2}k)]^{1/2}$$

$$-\frac{\pi}{2} \le \frac{\sqrt{3}a}{2}k \le \frac{\pi}{2}$$

Example : 1-D Band structure for a armchair CNT (5,5):

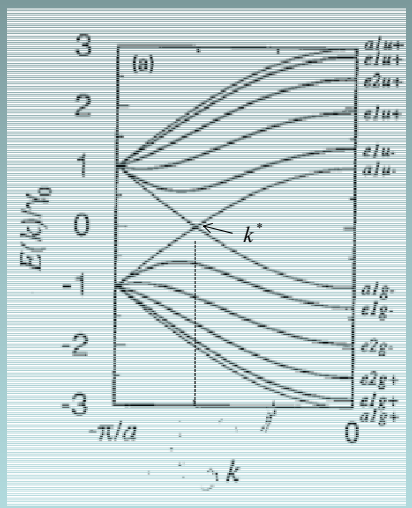

$$\therefore E^{1D}{}_{arm}(k_x = k, k_y = 2\pi q/15a)$$

$$= \sum_{q=1}^{5} \pm t[1 \pm 4\cos(\frac{\sqrt{3}a}{2}k)\cos(\frac{q\pi}{5}) + 4\cos^2(\frac{\sqrt{3}a}{2}k)]^{1/2}$$

$$-\frac{\pi}{2} \le \frac{\sqrt{3}a}{2}k \le \frac{\pi}{2}$$

- Conduction bands and valence bands each has
  4 doubly degenerate bands
  2 non-degenerate bands
- Band cross at k* : metallic conduction

$$k^* = (\frac{2\pi}{3\sqrt{3}a}, \frac{2\pi}{3a})$$

One of the Dirac point in 2-D band !!

1-D Band structure for a zigzag CNT (N_x,0):

2-D graphene sheet

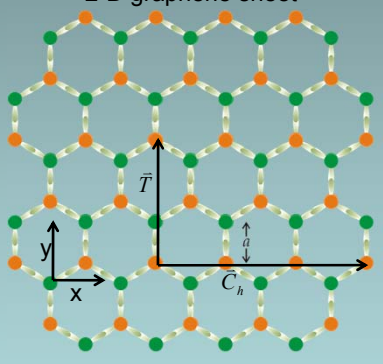

- In 1D zigzag CNT :

  k_x satisfy periodic boundary condition

$$\because k_x\sqrt{3}aN_x = 2\pi q$$

$$\therefore E^{1D}{}_{zigzag}(k_y = k)$$

$$= \sum_{q=1}^{N_x} \pm t[1 \pm 4\cos(\frac{3a}{2}k)\cos(\frac{q\pi}{N_x}) + 4\cos^2(\frac{q\pi}{N_x})]^{1/2}$$

$$-\frac{\pi}{2} \le \frac{3a}{2}k \le \frac{\pi}{2}$$

Example : 1-D Band structure for a zigzag CNT (9,0):

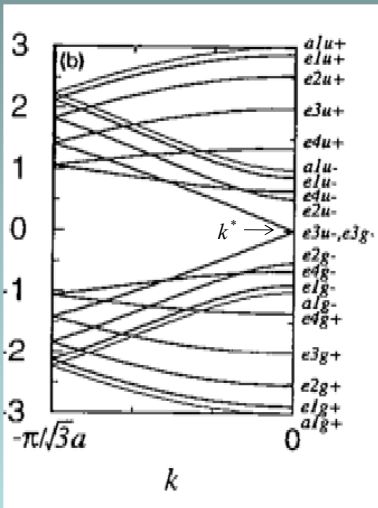

$$\therefore E^{1D}{}_{zigzag}\,(k_x = 2\pi q / 9\sqrt{3}a, k_y = k)$$

$$= \sum_{q=1}^{9} \pm t[1 \pm 4\cos(\frac{3a}{2}k)\cos(\frac{q\pi}{9}) + 4\cos^2(\frac{q\pi}{9})]^{1/2}$$

$$-\frac{\pi}{2} \le \frac{3a}{2}k \le \frac{\pi}{2}$$

- Conduction bands and valence bands each has
  8 doubly degenerate bands
  2 non-degenerate bands
- Band cross at k* : metallic conduction

$$\boxed{k^* = (\frac{4\pi}{3\sqrt{3}a}, 0)}$$

Another Dirac point in 2-D band !!

Example : 1-D Band structure for a zigzag CNT (10,0):

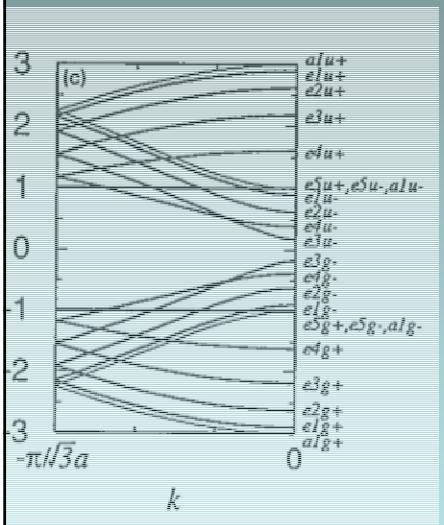

$$\therefore E^{1D}{}_{zigzag}\,(k_x = 2\pi q / 10\sqrt{3}a, k_y = k)$$

$$= \sum_{q=1}^{10} \pm t[1 \pm 4\cos(\frac{3a}{2}k)\cos(\frac{q\pi}{10}) + 4\cos^2(\frac{q\pi}{10})]^{1/2}$$

$$-\frac{\pi}{2} \le \frac{3a}{2}k \le \frac{\pi}{2}$$

- Conduction bands and valence bands each has
  9 doubly degenerate bands
  2 non-degenerate bands
- No Band crossing : semiconducting transport !!

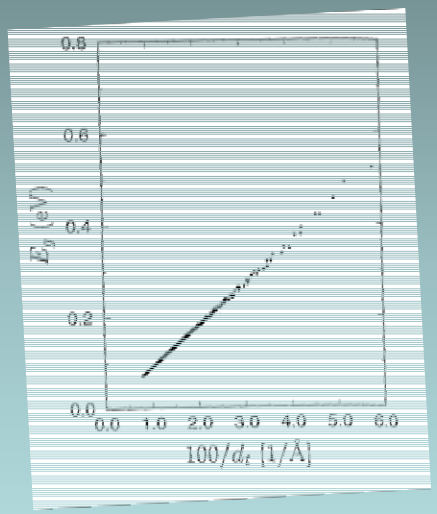

- Semiconducting CNTs:
  Band gap E_g depends on the tube diameter d_t but independent of chiral angle θ

$$E_g = \frac{ta}{d_t} \propto \frac{1}{d_t}$$

Slicing a 2-D graphene band

- alternative way of looking at 1-D Band in CNT

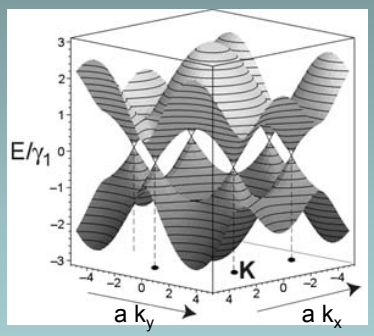

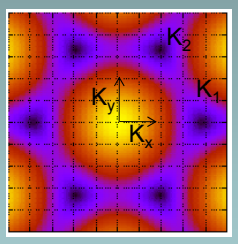

$E(\vec{q} = \vec{K}) = 0$

6 Dirac points

$$K_1 = \frac{4\pi}{3\sqrt{3}a}(1,0)$$

$$K_2 = \frac{4\pi}{3\sqrt{3}a}\left(\frac{1}{2}, \frac{\sqrt{3}}{2}\right)$$

- Whenever slicing through a Dirac point : metallic conduction
  otherwise : semiconducting transport behavior !

q=5

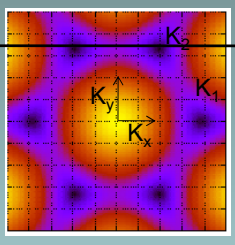

Armchair CNT (5,5):

$$\because k_y = \frac{2\pi q}{15a} \quad , -\frac{\pi}{\sqrt{3}a} \le k_x \le \frac{\pi}{\sqrt{3}a}$$

q=1,2…5

Slice through K_2 for q=5

➡ Metallic conduction

$$K_1 = \frac{4\pi}{3\sqrt{3}a}(1,0)$$
$$K_2 = \frac{4\pi}{3\sqrt{3}a}(\frac{1}{2},\frac{\sqrt{3}}{2})$$

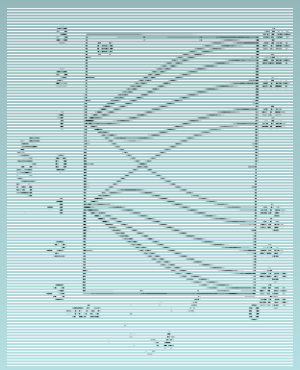

q=4

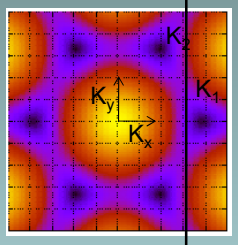

Zigzag CNT (10,0):

$$\because k_x = \frac{\pi q}{5\sqrt{3}a} \quad , -\frac{\pi}{3a} \le k_y \le \frac{\pi}{3a}$$

q=1,2…10

Does not Slice through any Dirac points

➡ Semiconducting transport behavior

$$K_1 = \frac{4\pi}{3\sqrt{3}a}(1,0)$$
$$K_2 = \frac{4\pi}{3\sqrt{3}a}(\frac{1}{2},\frac{\sqrt{3}}{2})$$

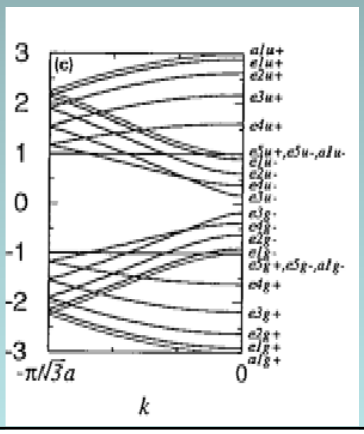

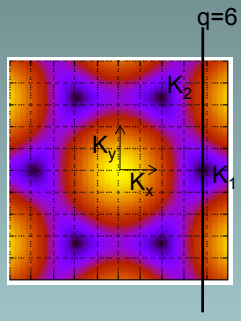

Zigzag CNT (9,0):

$$\because k_x = \frac{2\pi q}{9\sqrt{3}a} \quad , -\frac{\pi}{3a} \le k_y \le \frac{\pi}{3a}$$

q=1,2…9

Slice through K_1 for q=6

⇨ Metallic conduction

$$K_1 = \frac{4\pi}{3\sqrt{3}a}(1,0)$$
$$K_2 = \frac{4\pi}{3\sqrt{3}a}(\frac{1}{2},\frac{\sqrt{3}}{2})$$

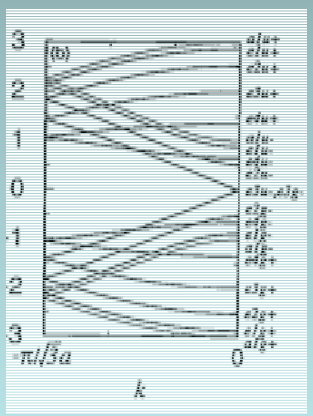

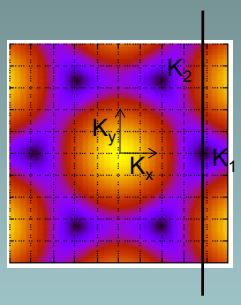

Zigzag CNT (N_x,0):

$$\because k_x = \frac{2\pi q}{N_x\sqrt{3}a}$$

q=1,2…N_x

- N_x : multiple of 3
  always Slice through K_1

⇨ 1/3 of Zigzag tube is metallic !!

$$K_1 = \frac{4\pi}{3\sqrt{3}a}(1,0)$$
$$K_2 = \frac{4\pi}{3\sqrt{3}a}(\frac{1}{2},\frac{\sqrt{3}}{2})$$

In general, metallic for n-m = multiple of 3
Magic number "3" in CNTs !!

Triangular lattice

"Applications of carbon nanotube

• Ambipolar Field-effect transistor (FET)

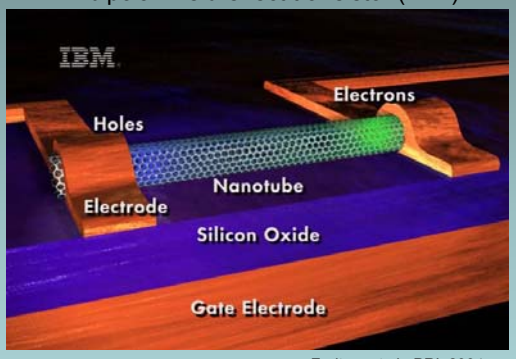

Freitag, et al., PRL 2004

Gate voltage sweep →

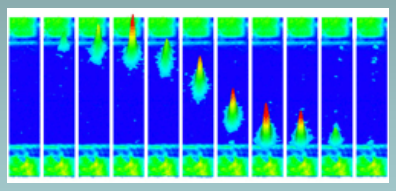

Color code : light intensity

• Fast switching time and large field-effect on the conductivity of the CNTs
• Infrared light emitters inside the nanotube

Part III: Concluding remark

• Label for a CNT (n,m)

• Mass production of CNTs using plasma enhanced CVD

• 1-D band structure of CNTs : slicing 2-D band structure of graphene

• 1/3 of the CNTs with random (n,m) is metallic.

• Application : CNT FETs, chemical sensors,
Fuel cell storage medium, mechanical reinforcement

Summary

0D - Fullerene

- Fullerene structure : C_{20+h*2}
- An example of strongly correlated electronic system
  Insulator – undoped C_{60}
  Metallic – Alkali-doped C_{60}
  Superconductivity – A_3C_{60} (A=K, Rb,CsK,RbCs)
- T_c increase linearly with lattice constant : BCS theory prediction

1D - Carbon nanotube

- Label for a CNT (n,m), 1/3 of the CNTs with random (n,m) is metallic.
- 1-D band structure of CNTs : slicing 2-D band structure of graphene
- Application : CNT FETs, chemical sensors,
  Fuel cell storage medium, mechanical reinforcement

2D - Graphene

- Chiral Fermionic excitation in single layer and bilayer graphene
- Unconventional QHE
- Phase coherent transport at the Dirac point
- Appearance of band gap in graphene nanoribbon, $E_g \sim 1/W$
- Novel phase near CNP at spin-polarized QH regime